

A Numerical and Statistical Analysis of the Fractured Rock Aquifer System in Ploemeur,  
France to Quantify Local and Regional Recharge

Stacey E. Law

Thesis submitted to the faculty of the Virginia Polytechnic Institute and State University  
in partial fulfillment of the requirements for the degree of

Master of Science  
In  
Geosciences

Thomas J. Burbey (Chair)  
Ryan M. Pollyea  
Laurent Longuevergne

June 11, 2019  
Blacksburg, VA

Keywords: hydrogeology, Ploemeur, vadose zone, fractured rock aquifer, recharge

Copyright © 2019, Stacey E. Law

# A Numerical and Statistical Analysis of the Fractured Rock Aquifer System in Ploemeur, France to Quantify Local and Regional Recharge

Stacey E. Law

## ABSTRACT

Groundwater recharge is an essential metric for understanding and protecting groundwater resources. Quantifying this parameter remains extremely challenging due to the uncertainties associated with the extent to which the vadose zone affects groundwater movement and the highly heterogeneous nature of the aquifer systems being monitored. The difficulty surrounding recharge quantification is compounded when considering a fractured rock aquifer system, where classification and modeling is complicated by highly complex structural geology. However, the ability to distinguish the character and geometry of fractured rock aquifers is indispensable for quantifying recharge to evaluate sustainable yields, as well as for implementing protective measures to manage these systems.

The primary intention of this study is to assess the hydrogeologic properties that have led the unique recharge signals within the fractured crystalline-rock aquifer system near Ploemeur, France. Infiltration and groundwater movement are characterized via time-series hydraulic head and precipitation data collected at daily, monthly, yearly, and at decadal intervals. In spite of the nearly one million cubic meters of groundwater extraction, measured drawdowns are marginal, suggesting that local and regional recharge plays a significant role in moderating water-level declines and raising questions as to the origins of the substantial inflow required to sustain this complex system. A roughly two-month lag has been observed between seasonal water level and monthly precipitation at Ploemeur, which has previously been attributed solely to slow vertical migration of water through the low-permeability micaschist layer to the fractured contact zone and interconnected fault.

However, results from this study suggest that a significant portion of the observed lag can be attributed to vadose-zone processes, particularly the thickness of the vadose zone. This investigation also reveals a recharge signal that continues throughout the calendar year, departing from the traditional simplified concept that recharge quantity is essentially equivalent to the value of evapotranspiration subtracted from infiltration.

A Numerical and Statistical Analysis of the Fractured Rock Aquifer System in Ploemeur,  
France to Quantify Local and Regional Recharge

Stacey E. Law

GENERAL AUDIENCE ABSTRACT

Groundwater recharge is the amount of water added to underground water sources, called aquifers. This occurs as precipitation falls to the ground, moves downward through the unsaturated subsurface, and accumulates at the top of the saturated zone, deemed the water table. The saturated zone is so named because all pore spaces between sediment grains or crevices in rocks are fully filled with water. Understanding groundwater recharge is important to the protection of groundwater resources, but is hard to estimate due to the lack of knowledge about water movement in the unsaturated zone and the uncertainties related to the systems being studied. Aquifers forming within fractured rocks are even more challenging to investigate, because the complex geological structures are difficult to replicate with computer modeling. However, fractured rock aquifers are an important groundwater resource, and understanding them is the first step in estimating recharge within the system. Recharge estimates are used to calculate how much water can be safely removed from the aquifer for years to come, so that the resource can remain protected.

The aim of this investigation is to assess the aquifer properties that lead to the unique recharge signal in a fractured crystalline-rock aquifer in Ploemeur, France, where nearly 1 million cubic meters of water have been removed each year since 1991 but water table levels have not fallen significantly. This behavior raises questions about the water returned to the system as recharge that is sustaining such a highly productive resource. This site also shows a roughly two-month lag between seasonal precipitation falling and the

reflection of that precipitation recorded in the water level of the aquifer. It was previously thought that the lag occurred because water travelled slowly through the mica-schist layer, which has little pore space for water to move, and into the contact zone and interconnected fault. However, this study shows instead that a majority of the lag is associated with the unsaturated zone properties and processes, particularly thickness. This investigation also shows recharge entering the aquifer system throughout the calendar year, a departure from earlier studies conceptualizations.

## Acknowledgements

I would first like to thank my advisor, Dr. Thomas Burbey, for taking me on as both a student and a teaching assistant and providing me the opportunity to work on such an interesting and challenging project. I deeply appreciate his support and assistance in adapting a portion of this large-scale investigation to fit the scope of my time at Virginia Tech, and I will always be grateful for his classes that completely changed my opinion of MATLAB (for the better).

I am very grateful to my committee members Dr. Ryan Pollyea and Dr. Laurent Longuevergne for their invaluable feedback during my annual reviews, and for generously lending their time, expertise, and perspectives to this project.

I am appreciative of the funding and support received from the National Science Foundation and the Geosciences Department at Virginia Tech that made this work possible and supported my continued education. This department and its incredible professors, students, and administrators gave me innumerable opportunities for growth and pushed the boundaries of my personal and professional development, and for that I give all of my thanks.

Finally, my journey through grad school would not have been possible without my support system. To Mom, Dad, and Trish, for cheering me on from up in PA and giving me the freedom and confidence to venture a little farther from home; and to my friends both in and outside of grad school, for the phone calls, hikes, and happy hours in between the hard work. Thank you for struggling and celebrating and learning alongside me – I'm thankful that I got to climb these mountains with you.

## Table of Contents

Abstract .....	ii
General Audience Abstract .....	iv
Acknowledgements .....	vi
Introduction .....	1
Recharge Mechanisms .....	1
Vadose Zone Processes and Properties .....	6
Fractured Rocks and Recharge .....	9
Hydrogeologic Site Description .....	11
Methods .....	16
Unsaturated Zone Flow Model Theory .....	16
Model Construction and Calibration .....	19
Statistical Analysis Using MATLAB .....	23
Results & Discussion .....	29
Vadose Zone Thickness & Temporal Recharge Distribution .....	29
Spatial Distribution of Recharge .....	33
Seasonal Recharge Quantification .....	34
Uncertainty .....	41
Conclusions .....	42
References .....	44

## List of Figures

Figure 1: <i>Conceptual example of fractured flow in the context of the Ploemeur aquifer site</i> .....	5
Figure 2: <i>Seasonal signals seen in precipitation (dark blue) and hydraulic head measurements at the Ploemeur site</i> .....	6
Figure 3: <i>Location of the Ploemeur hydrogeological site</i> .....	12
Figure 4: <i>Block diagram representing the details of the underlying structure and geology at the Ploemeur site</i> .....	13
Figure 5: <i>A simple conceptual diagram of vertical unsaturated flow vs more dynamic saturated flow</i> .....	17
Figure 6: <i>Plan view of model, showing gridded area and well locations geo-coded over a GoogleEarth satellite image of Ploemeur</i> .....	20
Figure 7: <i>Displaying the average daily hydraulic head values at intervals during the calendar year</i> .....	24
Figure 8: <i>A mathematical conceptualization of the study site</i> .....	25
Figure 9: <i>Distributions of the three tests run using the quantification model</i> .....	26
Figure 10: <i>Highlighting the values from the model output used in calculating the monthly sums of infiltration, recharge, and ET</i> .....	27
Figure 11: <i>The effect of varying unsaturated zone thickness on recharge quantity</i> .....	30
Figure 12: <i>Vadose thickness in January, April, August, and December (clockwise from upper left:)</i> .....	32
Figure 13: <i>The spatial distribution of recharge</i> .....	34
Figure 14: <i>Simulated measurements of infiltration, UZF recharge, and UZF ET quantities (blue, orange, and gray, respectively)</i> .....	35
Figure 15: <i>Plot showing the amount of simulated head change in 10 of the observation wells at Ploemeur</i> .....	36
Figure 16: <i>Sensitivity of input parameters in relation to evapotranspiration simulation</i> .....	37



Figure 17: *Locations of the wellsites used exclusively for this study (purple squares), the wellsites used exclusively in the investigation conducted by Jimenez et al., 2013 (yellow squares), and wellsites used in both studies (blue stars) ..... 40*

## List of Tables

Table 1: <i>Showing the input values for the Unsaturated Zone Flow package as they were entered for one year of run time</i> .....	21
Table 2: <i>Lengths of modeled time necessary for UZF recharge to attain a given cumulative quantity in cells with each of the plotted thicknesses</i> .....	31
Table 3: <i>Graph showing the total monthly simulated quantities for the indicated UZF parameters over the 36 months of simulation time</i> .....	39

## **Introduction**

### RECHARGE MECHANISMS

Groundwater recharge can be simply defined as the quantity of water supplementing a groundwater reservoir. Recharge is the foremost constraint in qualifying the accessibility and maintainability of groundwater resources; thus, it is crucial to calculating sustainable yields (*Ali et al., 2017*). In conjunction with discharge and groundwater flow velocities and directions, this data is used to establish groundwater budgets in aquifer systems (*Cook, 2003*). Recharge can occur directly, as precipitation infiltrates vertically through the system; or indirectly, as from runoff, preferential accumulation in joints, ponding in topographically low areas, or leakage from surficial water bodies (*Lloyd, 1986*).

While meteoric water is a common source of recharge, alternate origins include surface water such as lakes and streams; irrigation flow; snowmelt; and urban recharge. Lakes and streams can lose water to groundwater bodies through seepage when the water table is lower than the surface water level; this outflow can occur throughout either the entire bed or partial sections of bed depending on water table elevation (*Winter et al., 1998*). Irrigation return flow has been observed to recharge groundwater, especially in areas with dry seasons, as water relocated and utilized for farming re-enters the subsurface (*Mustafa et al., 2017*). Shallow groundwater systems in areas with seasonal snowpack experience a spike in recharge during spring melt times; indeed, this is the foremost recharge stage for many catchment networks (*Flerchinger et al., 1991; Sklash and Farvolden, 1979; Rodhe, 1987*). Buttle and Sami (*1990*) suggested that this source of groundwater was most effective in areas with water tables as shallow as 1 meter or less

below the land surface. Urban recharge comprises leaks from infrastructure in place for water supply and sewage networks, with the former responsible for the bulk of the supplemental recharge (*Lerner, 2002; H.B. Wakode et al., 2018*).

Water that infiltrates at ground surface moves through the subsurface vertically as potential recharge; it percolates towards the water table to become groundwater in the saturated zone, where flow is both vertical and lateral (*Winter et al., 1998*). However, movement specifically related to recharge can exhibit more variety, spanning from piston flow and preferential flow paths to inter-aquifer flow and diffuse recharge. Piston flow occurs as newer recharge from the surface downwardly displaces water that had been formerly stored in the unsaturated zone (*Hewlett and Hibbert, 1967; Zimmermann et al., 1967; Buttle and Sami, 1990*). The concept is that mass water movement is layered, with recharge waters from different years/precipitation events stacked above one another; this is more commonly observed in more homogenous soils (*Zimmermann et al., 1967; Sukhija et al., 2003*). Preferential flow paths are often observed in aquifers set within faulted, fractured or jointed media, resulting from interconnected fracture orientations that allow water to flow through multiple linked channels within a lower-permeability matrix (*Gleeson et al., 2009; Pedretti et al., 2016; Roques et al., 2016; Schuite et al., 2017*). Recharge in such systems is influenced by a variety of factors, including the connectivity and size of fracture openings (*Gleeson et al., 2009; Cook, 2003*). Interaquifer flow, also described as groundwater underflow, occurs as leakage across a semi-permeable layer separating two aquifers (*Eko, 2013; Healy, 2010*). This is not always strictly considered recharge, but still falls under the umbrella term and must be taken into account as part of the water balance of an aquifer (*Lerner, 1990*). Finally, diffuse recharge refers to

precipitation over a large spatial extent that infiltrates through the unsaturated zone to the water table, a method that dominates humid regions (*Healy, 2010*).

Accurately estimating groundwater recharge is essential for proper management of groundwater resources; however, a multitude of challenges face proper quantification of this important process. The foremost issue is that recharge is almost impossible to directly and completely measure, and the most precise methods for subsurface data collection are expensive and complex (*Lerner et al., 1990; Scanlon et al., 2002*). Natural heterogeneity in soil permeability, vegetation, and geologic material are overarching spatial complications in recharge calculations, and temporal complications arise with seasonal, decadal, or long-term climatic signals (*Healy, 2010*). Additionally, there are a variety of occurrences that can influence water table fluctuations without representing true groundwater recharge, such as air entrapment during recharge, bank-storage effects near streams, tidal effects near oceans, pumping, and deep-well injections (*Freeze and Cherry, 1979*).

In an effort to combat these issues, a variety of approaches are used to quantify groundwater recharge using more easily measured parameters, such as soil moisture content, hydraulic head fluctuations, hydraulic conductivity, and evapotranspiration and extinction depth (*Lerner et al., 1990; Healy, 2010; Ali et al., 2017*). The water table fluctuation method is also an option, as successfully demonstrated by Lee et al. (2006). This method involves the use of high-resolution (i.e. daily or hourly) groundwater level data combined with numerical modelling of matrix and fracture flow within the aquifer material as a way of designing recharge models (*Lee et al., 2006*).

Errors commonly occur when estimates of precipitation and evapotranspiration (ET) are erroneously high, a mistake that is generally noticed regarding arid and semi-arid sites (*Gee and Hillel, 1988; Sukhija, 2003*). ET quantification presents a challenge because the most frequently used methods calculate potential ET, which is the highest amount of water that could be removed under the most favorable conditions if said amount of water was available in the system. However, actual ET measurements are reliant on unsaturated soil storage properties and vegetation, as opposed to the atmospheric properties that govern potential ET, leading to higher and more common errors in ET measurement and subsequently, recharge estimation (*Freeze and Cherry, 1979*). Recharge estimates based solely on soil hydraulic conductivity and texture can also often be incorrect, as even small changes in spatial variability of soil can produce large effects on infiltration (*Freeze and Banner, 1970; Freeze and Cherry 1979*).

Fractured rock aquifer systems require particular attention, as many traditional methods of calculating recharge do not apply due to the level of heterogeneity present. Flow rates for aquifers in porous media are estimated by Darcy's Law; while this method is still technically available for fractured rock aquifers, a complication arises in the excessive level of variability shown in the hydraulic conductivities and the anisotropy caused by preferential fracture orientation (*Cook, 2003; Farkas-Karay et al., 2015*). These preferential flow paths [Figure 1] that exist in fault-deformed fractured rock complicate the study of recharge patterns. At the local scale, recharge in such systems is influenced by a variety of factors, including the connectivity and size of fracture openings, topography, soil attributes, vadose thickness, and hydraulic gradients (*Harte and Winter, 1996; Gleeson et al., 2009*).

The aquifer system in Ploemeur, FR is unusually prolific for a crystalline aquifer, producing exceptionally high yields ( $10^6 \text{ m}^3 / \text{yr}$ ) while exhibiting remarkably small drawdowns ( $\sim 10 - 20$  meters).

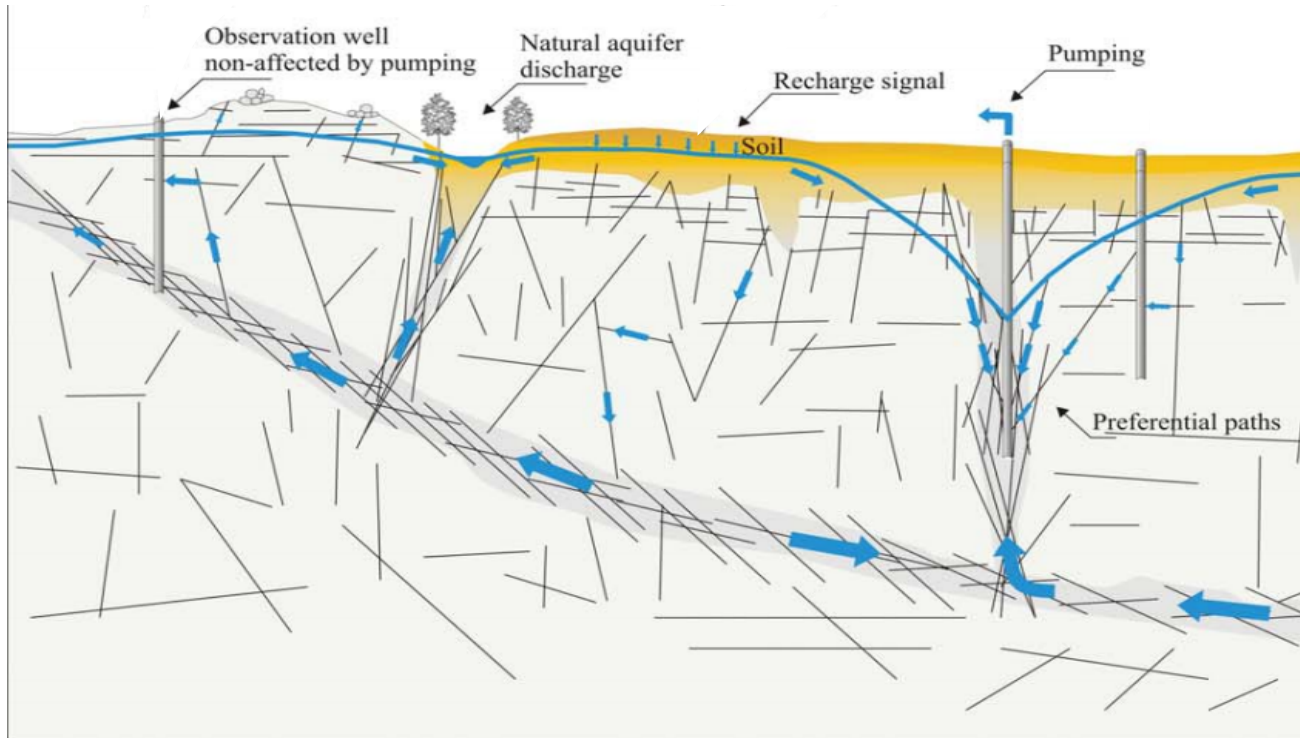


**Figure 1.:** *Conceptual example of fractured flow in the context of the Ploemeur aquifer site; preferential flow paths are clustered around the contact zone (deeper flow, horizontal arrows) and the fractured fault zone (pumping area to the right, vertical arrows) Note that this image does not represent flow dynamics specific to the Ploemeur site (Modified from Jimenez et al., 2013).*

These patterns occur in a structure that would normally have low storage and permeability values, raising questions about the recharge signal that supplies the fractured system.

We also observe a lag between precipitation events and water-table response, on the scale of approximately two months [Figure 2]. Precisely constrained, the maximum precipitation generally occurs on November 12th, while head values generally peak on

April 3<sup>rd</sup> of the year following, exhibiting a lag of 145 days. The primary objective of this study is to evaluate the properties constraining recharge and the lag between hydraulic head and precipitation by using numerical and statistical techniques to analyze groundwater transport within the vadose zone and quantify seasonal recharge estimates.

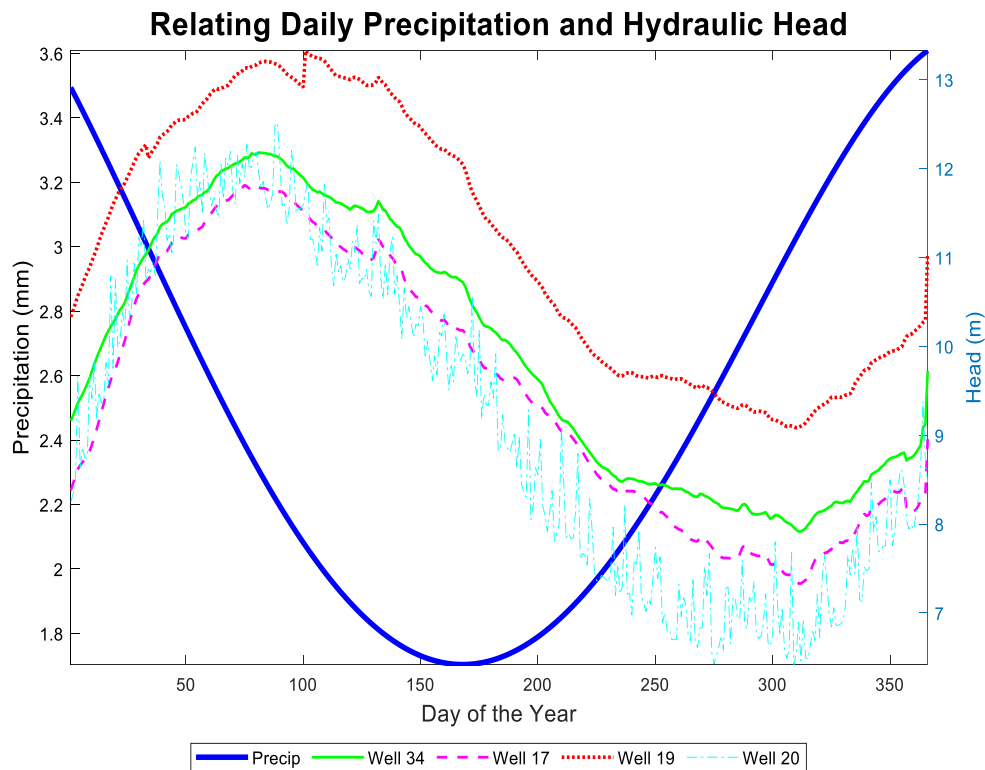


**Figure 2.:** Seasonal signals seen in precipitation (dark blue) and hydraulic head measurements at the Ploemeur site. Wells were chosen due to similar head ranges, to best manage the scope of the y-axis scale and exhibit the lag time between maximum precipitation occurrence and subsequent reflection in the water column.

## VADOSE ZONE PROPERTIES AND PROCESSES

The unsaturated zone is one of the least understood elements within the hydrologic cycle (Gee and Hillel, 1988; Buttle and Sami, 1990). Sometimes called the vadose zone, or the aerated zone, this expanse constitutes the zone of subsurface between land surface and water table, which is the upper limit of the saturated zone (Haverkamp et al., 2006;



*Bouwer, 1978; Freeze and Cherry, 1979*). The variety in its natural components, ranging from soil and rocks to air, plants, and water makes this zone highly complex, and interactions among these various constituents must be taken into account in unsaturated zone hydrology (*Nimmo, 2005*). The various scales at which vadose processes take place – micro, macro, and megascale – add further complexity to the parameterization of unsaturated dynamics (*Haverkamp et al., 2006*). The impact of vadose zone hydrology has historically been passed off or greatly simplified, due to limited data availability or difficulty. However, a conceptualization of unsaturated flow is essential to understanding recharge dynamics, as the rates, timing, and patterns of aquifer recharge are controlled by unsaturated processes and properties (*Cassiani et al., 2007*).

The unsaturated zone can be broken into three subsections: the upper root zone, the intermediate zone, and the capillary fringe. The root zone tends to exist on the scale of a few meters, and is defined by the depth reached by plant roots (*Guymon, 1994; Hornberger et al., 1998*). The capillary fringe exists just above the water table, where capillary forces draw water upward from the water table. The thickness of this zone is pore-size dependent, with an inverse relationship existing between pore size and fringe breadth; fine-grained materials exhibit capillary zones multiple meters in thickness, whereas coarse-grained soils have only a centimeter or so of capillary fringe (*Tolman, 1937; Guymon, 1994*).

The vadose zone is the connection between surface water and groundwater, and hosts a number of key exchanges between the subsurface, surface water, and the atmosphere (*Cassiani et al., 2007; Haverkamp et al., 2006*). The unsaturated zone gains water via infiltration of precipitation and surface water, and loses water through evaporation, evapotranspiration, and drainage (*Haverkamp et al., 2006*). As water at the

surface infiltrates the ground, it has been shown to move at a rate that decreases with time; any given soil has a limiting curve defining the maximum rate of infiltration vs. time. As water accumulates, the capacity of the unsaturated zone to hold more moisture decreases, and ultimately the rate of infiltration approaches a constant rate (*Freeze and Cherry, 1979*). Evapotranspiration is a process of water removal that depends on soil moisture, atmospheric conditions, and type of vegetation. When water is abundant, atmospheric conditions are the limiting factor in the amount of water uptake, but rates decrease in drier periods even if atmospheric conditions remain the same, in order to regulate the flow of water to plant roots (*Hornberger et al., 1998*).

Traditional unsaturated flow theory examines two types of factors to determine water movement: driving forces, such as gravity and matrix pressure; and material properties, including storage and hydraulic conductivity (*Nimmo, 2005; Cassiani et al., 2007*). Another essential property to vadose flow is the volumetric moisture content, represented in equations as  $\theta$  and defined as the decimal fraction  $\frac{\text{Volume (water)}}{\text{Volume (total)}}$ . In unsaturated flow,  $\theta$  is always less than the porosity. Total volume is the complete unit volume of a soil or rock, and is comprised of the volume of the solids ( $V_s$ ), water ( $V_w$ ) and air ( $V_a$ ) (*Freeze and Cherry, 1979*).

Water movement in unsaturated porous media is treated as one-dimensional vertical flow, defined by the continuity equation

$$\frac{\partial \theta}{\partial t} = \frac{\partial q}{\partial z} \quad (1)$$

where  $\theta$  is volumetric soil water content;  $q$  is water flux,  $z$  is depth (positive downward), and  $t$  is time. In combination with Darcy's Law, which describes fluid flow through porous media as:

$$q = -K(\theta) \frac{\partial H}{\partial z} \quad (2)$$

the equation can be written as

$$\frac{\partial \theta}{\partial t} = \frac{\partial}{\partial z} \left[ K(\theta) \left( \frac{\partial h}{\partial z} - 1 \right) \right] \quad (3)$$

where  $h$  is soil water pressure head and  $K$  is hydraulic conductivity (*Darcy, 1856; Haverkamp et al., 2006*). An alternative form of transient vadose flow that depends on hydraulic soil diffusivity is based around a variation to Richards' equation, yielding:

$$\frac{\partial \theta}{\partial t} = \frac{\partial}{\partial z} \left[ D(\theta) \frac{\partial}{\partial z} (\theta) \right] \quad (4)$$

This equation requires the assumption that flow is driven by water content gradients, as opposed to potential.  $D(\theta)$  is a material property dependent on soil water content, and can be easier to measure and less variable than  $K(\theta)$  (*Childs and Collis-George, 1950; Nimmo, 2005*).

#### FRACTURED ROCKS AND RECHARGE

Igneous and metamorphic rocks typically are not associated with high primary porosity or permeability due to their close crystalline structure, and therefore are not ideal

candidates for reservoir formation. In spite of this reality, groundwater stored in crystalline rock constitutes an essential resource, considering approximately one-third of continental crust surface is comprised of igneous and metamorphic rock (*Blatt and Jones, 1975; Amiotte-Suchet et al., 2003; Gleeson et al., 2012*). However, there is a dearth of knowledge concerning sustainable yield from these aquifers due to the difficulty of estimation based on the heterogeneous nature of crystalline basement. The ability of crystalline aquifers to conduct a productive amount of water is dependent on the presence of fractures in the system (*Berkowitz, 2002; Stober and Bucher, 2006; Roques et al., 2016*). Rocks characterized by low primary porosity and permeability are more prone to brittle deformation and therefore are better candidates for conductive fracturing. The network of fractures must be dense and exhibit interconnectivity in order to be considered prolific; to be classified as a ‘fractured rock aquifer’, a rock mass must demonstrate groundwater flowing in usable quantities, a qualification which spans a range of discharge amounts depending on the intended use of the resource (*Pedretti et al., 2016; Lamur et al., 2017*). Alignment, length, spatial arrangements and density are used to geometrically classify such fracture complexes (*Pedretti et al., 2016*).

Aquifers in plutonic and metamorphosed rock are typically limited to the upper ~50 m, where there is improved connectivity of fractures from jointing and weathering in addition to increased permeability compared to lower depths affected by overburden stress (*Dewandel et al., 2012; Roques et al., 2016*). Fracture connectivity is determined by examining the ratios of the different types of fracture extinctions observed within the system. These terminations include fractures termed ‘blind’, as they end within the rock matrix; fractures that intersect additional fractures; and fractures that border others (*Cook,*

2003). The spatial configuration of the fractures, and thus of the flow paths, determines the level of influence that scale exerts on the hydraulic properties. Flow in fractured media is directed by head gradients, and is often localized within a small number of preferential flow paths (Roques *et al.*, 2016). Average bulk permeability values in crystalline bodies are exceptionally small, ranging between  $10^{-15} - 10^{-17} \text{ m}^2$  (Le Borgne *et al.*, 2007; Gleeson *et al.*, 2011; Schuite *et al.*, 2017).

Greatly transmissive fractures in crystalline rock are frequently related to fault zones, as fault movement elicits the formation of a higher-permeability fractured reservoir within the low permeability basement (Roques *et al.*, 2016). The term ‘fault zone’ is considered to describe a body of rock in which permeability has been affected by fault-driven deformation (Bense *et al.*, 2013). The governing law of porous-media fluid flow, Darcy’s Law, states that permeability and hydraulic gradient command subsurface flow. Hydraulic gradients associated with fault zones are strongly influenced by recharge rates that induce flow to follow topography, as well as anthropogenic processes such as pumping (Bense *et al.*, 2013). Structural components of fault zones, such as the dip of the feature, also have a tangible impact on yield. Flat-lying or gently dipping faults and structures are thought to be capable of providing more water resources, as they have a larger surficial extent available for recharge (Reulleu *et al.*, 2010).

#### HYDROGEOLOGIC SITE DESCRIPTION

The Ploemeur hydrogeological site is located in the southern area of the Brittany province in France [Figure 3], a low-lying area within 15 km of the coast with no more than 50 m of total elevation change. The site is situated within an oceanic climate, where

the mean precipitation is 900 mm/yr, the mean evapotranspiration demand is estimated at 750 mm/yr (Roques et al., 2018; Jimenez-Martinez et al., 2013). The region has been shaped by a number of syntectonic granitic intrusions into the overlying micaschist bedrock, and is located within the heavily faulted Armorican Massif. A quarter of the Brittany region's drinking water is supplied by groundwater sources, of which 40% is obtained from crystalline rock aquifers (Roques et al., 2016). One such aquifer, the focus of this study, is defined by a pair of structural features [Figure 4]; the first, a subvertical eastward-dipping normal fault striking N20°, spans between 100-150m in width and is the result of tectono-metamorphic events occurring in the Silurian and Devonian.

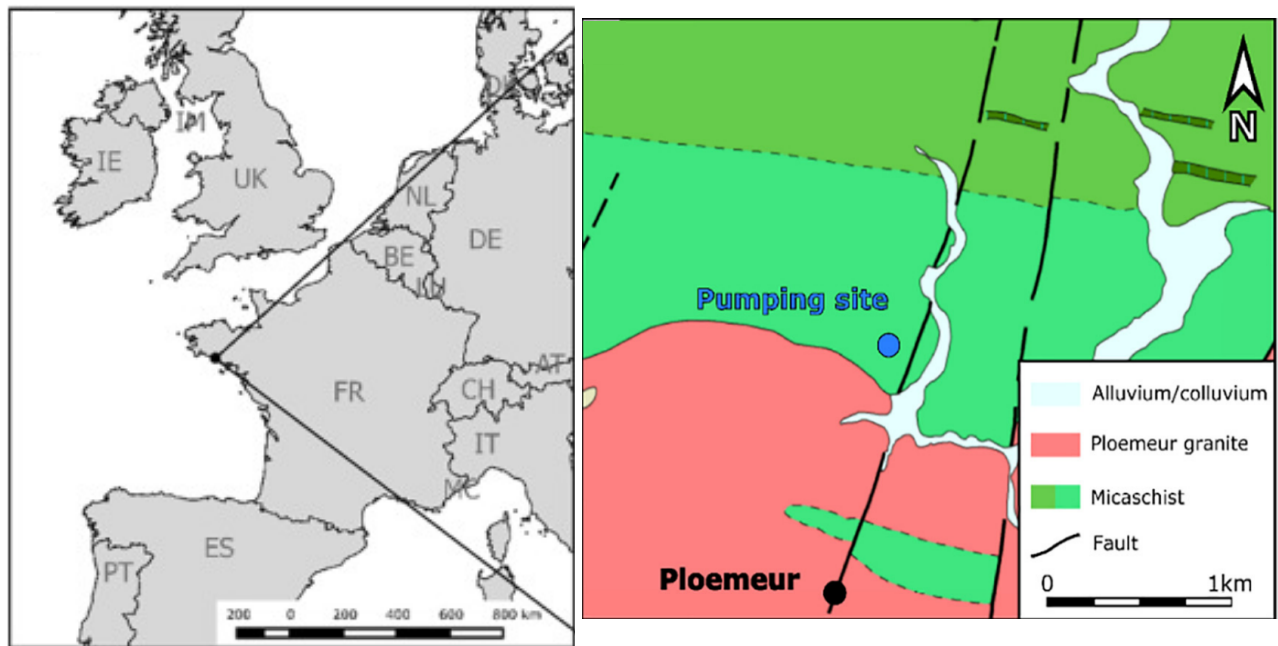


**Figure 3.:** Location of the Ploemeur hydrogeological site. Geographical context is shown to the left, while to the right lies a conceptual map of the underlying geology and structural components (Modified from Aquilina et al., 2018).

The micaschist exhibits ductile deformation, which increases in frequency towards the contact zone due to the granitic emplacement. The contact zone itself is distinguished by

expanses of micaschist intruded by granite dykes (*Le Borgne et al., 2006*). Overlaying the bedrock is a layer of lower permeability clayed and sandy regolith measuring from 10-30 m in thickness, with more developed weathering exhibited in the topographically low areas near the fault zone.

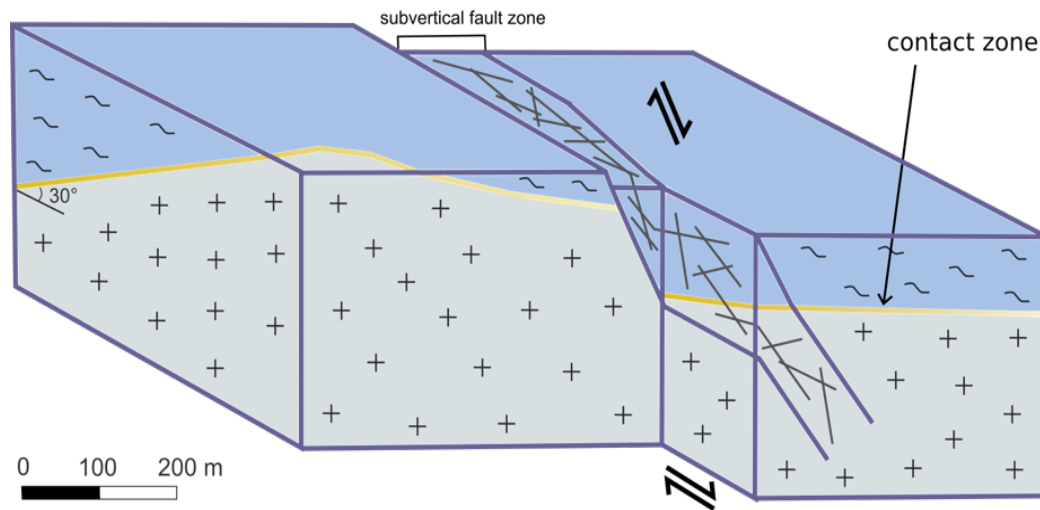


**Figure 4.:** Block diagram representing the details of the underlying structure and geology at the Ploemeur site. The contact zone between the granite (gray +) and overlying micaschist (blue ~) is shown in yellow; the subvertical normal fault and fractured fault zone is delineated between the two blocks to demonstrate tectonic movement (*Modified from Schuite et al., 2015*).

Localized flow is primarily restricted to this top layer due to the effective density and connectivity of the fracture array; here, the groundwater movement is northwest-to-southeast with a moderate hydraulic gradient of 5%. Deeper flow in the more permeable contact zone and fractured fault zone exhibits a longer residence time (50+ years) and preferential upward flow, as evidenced by higher hydraulic heads measured from boreholes intersecting these structures (*Aquilina et al., 2015; Roques et al., 2018*). These upward fluxes produced a natural discharge site prior to the exploitation of the aquifer (*Jimenez-*

*Martinez et al., 2013*). Upon installation, some wells were artesian due to these ambient upflows from differing heads in various fractures (*Le Borgne et al., 2004*).

The site is uncharacteristically productive, providing for the town's 20,000 residents with annual withdrawal rates from pumping wells within the fault zone nearing  $10^6$  m<sup>3</sup>/yr, or  $2.88 \cdot 10^6$  L daily (*Le Borgne et al., 2004*). Despite the high well yield, drawdown remains minimal at approximately 20 m (*Leray et al., 2013*). As part of the H+ hydrogeological network, the area has been monitored closely since its discovery in 1991 via a system of nearly fifty wells ranging from 30 m to 150 m in depth; three are pumping wells and the remainder are observation boreholes, screened for their entire length save the first 20-40m (*Roques et al., 2018*). Boreholes within a 600 m radius of the pumping wells consistently react cursorily to deviations in pumping, even after significant lapses in time (*Le Borgne et al., 2006*).

Wells at the site were preferentially drilled following the normal fault zone. Pumping tests show that the hydraulic response of the majority of the piezometers is associated with the normal fault zone, while the easternmost piezometers reflect properties of the contact zone. In the contact zone, hydraulic head variations occur more quickly and exhibit less drawdown than those in the fault zone. Calculations estimate that the generalized transmissivity of the contact zone is likely double that of the fractured fault zone, and with a corresponding storage coefficient that is between 2-7 times smaller.

These variations in hydraulic properties can be interpreted as differences in fracture density or fracture aperture, such that the properties of the fault zone suggest densely fractured area with relatively small apertures and the higher transmissivity of the contact zone suggests a more sparsely fractured area with larger apertures (*Le Borgne et al., 2004*).



The overall transmissivity of the site is comparatively higher than similar rocks in the province, on the scale of 86,400 L/day (*Le Borgne et al., 2007*). High transmissivity zones, indicative of strong interconnectivity of fractures acting as preferential flow paths, connect across distances of over 150 m at the Ploemeur site (*Le Borgne et al., 2006*).

## **Methods**

### *UNSATURATED ZONE FLOW MODEL THEORY*

The purpose of applying a vadose zone model is to determine contribution of the time lag between precipitation and the hydraulic head response attributed to percolation of water through the unsaturated zone. The goal of this model is to examine the seasonal recharge signal in relation to the thickness of the vadose zone by applying time-series precipitation, ET, and head data from the Ploemur site. We systematically work to understand the impact of the hydromechanical properties within the Ploemur system, beginning with an analysis of groundwater transport within the vadose zone. Model construction involved using the Unsaturated Zone Flow (UZF1) and the Time-Variant Specified-Head (CHD) packages in MODFLOW-2005 with ModelMuse (*Niswonger et al., 2006; Winston, R.B., 2009; Niswonger et al., 2011*). MODFLOW utilizes the finite-difference method by which the aquifer system is divided into cells by a grid of user-specified size; applied to those cells are user-designated hydraulic properties. This project largely involved forward modeling, which implements field observations as input parameters in order to model groundwater movement.

The UZF1 package was chosen for its ability to simulate water flow and storage in the unsaturated zone, allowing for determination of the extent to which the unsaturated zone influences water movement physically and temporally. This package works by using a kinematic wave approximation to Richard's equation as solved by the method of characteristics to represent the vertical movement of unsaturated flow, shown in [Figure 5] (*Niswonger et al., 2006*). Richard's equation is simplified in this package to:

$$\frac{\partial \theta}{\partial t} = \frac{\partial}{\partial z} \left[ D(\theta) \frac{\partial \theta}{\partial z} - K(\theta) \right] - i, \quad (5)$$

where

$\theta$  is volumetric water content

$q$  is water flux

$z$  is vertical depth

$D(\theta)$  is hydraulic diffusivity

$K(\theta)$  is unsaturated hydraulic conductivity as a function of water content

$i$  is ET rate per unit of depth

$t$  is time

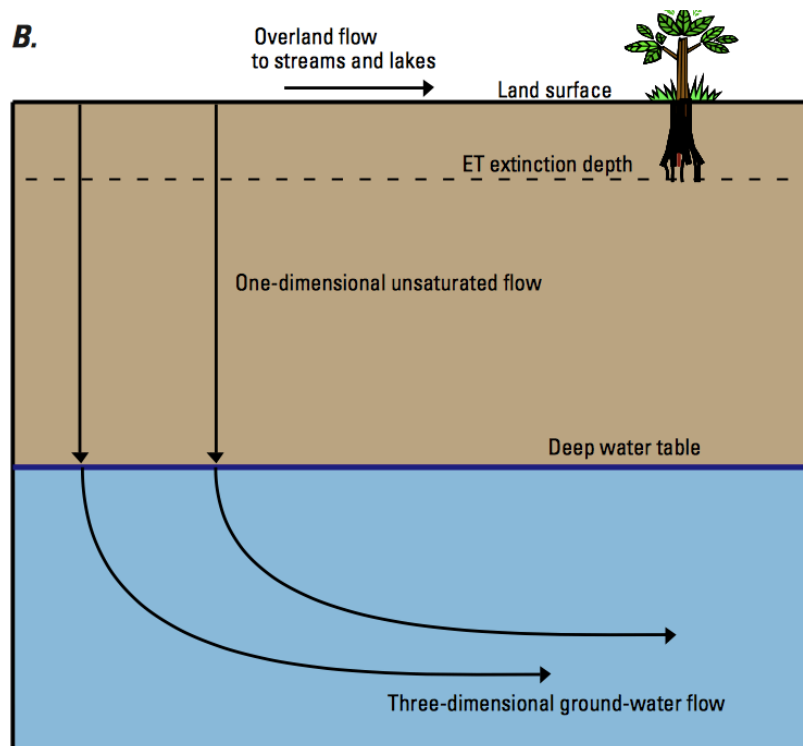


**Figure 5:** A simple conceptual diagram of vertical unsaturated flow vs more dynamic saturated flow, as modeled by the UZF1 package (modified from Niswonger et al., 2006).

An essential assumption to the approximation method is that gravitational forces are the only driving factor of vertical flux, meaning that the diffusive term is removed from the above equation. Further assumptions include evaporation being immediately removed

from the soil column and all flow is moving vertically downward. Incorporating these assumptions, the original equation is modified to:

$$\frac{\partial \theta}{\partial t} + \frac{\partial K(\theta)}{\partial z} + i = 0 \quad (6)$$

Water movement in the unsaturated zone occurs in waves designated as wetting and drying fronts; increased infiltration prompts formation of a wetting front, while a decrease prompts a drying front. To examine the wave of a wetting front, Eqn. 6 is rewritten as a partial derivative of  $\theta$  with respect to  $t$  and  $z$ , yielding:

$$\frac{\partial \theta}{\partial t} + \frac{\partial K(\theta)}{\partial \theta} \frac{\partial \theta}{\partial z} = -i \quad (7)$$

Combining Eqn. 7 with Abbott's equation of variation (1966):

$$\frac{\partial \theta}{\partial t} dt + \frac{\partial \theta}{\partial z} dz = d\theta, \quad (8)$$

the equation can be written in matrix form as

$$\begin{bmatrix} 1 & \frac{\partial K(\theta)}{\partial \theta} \\ dt & dz \end{bmatrix} \begin{bmatrix} \frac{\partial \theta}{\partial t} \\ \frac{\partial \theta}{\partial z} \end{bmatrix} = \begin{bmatrix} i \\ d\theta \end{bmatrix}, \quad (9)$$

which is then expanded into its determinants

$$\frac{\partial z}{\partial t} = \frac{\partial K(\theta)}{\partial \theta} = v(\theta) \quad (10a)$$

$$\frac{\partial \theta}{\partial t} = -i \quad (10b)$$

$$\frac{\partial \theta}{\partial z} = \frac{-i}{v(\theta)} \quad (10c)$$

where 10a represents the velocity of a wave in the unsaturated zone, 10b represents the change in water content of that wave over time, and 10c represents the change in water content with vertical distance following the wave.

The package simulates a one-dimensional plane over a three-dimensional saturated zone model, applying an infiltration rate at the model's land surface and removing evapotranspiration first from the unsaturated zone, and then from the groundwater reservoir if necessary. This diverges from the traditional 'Recharge' and 'Evapotranspiration' packages available in MODFLOW, which apply recharge directly to the water table and calculate the head-dependent evapotranspiration flux by removing ET from above the extinction depth first before moving to the reservoir if demand is not met, respectively (*Harbaugh, A.W., 2005; Niswonger et al., 2006*). UZF1 examines the difference between land elevation data values and hydraulic head values to approximate the unsaturated zone thickness at each cell. Mass balance is calculated via estimation of the residual water content, with specific retention calculated as specific yield subtracted from the saturated water content. The surface discharge is able to be routed to streams or lakes; in the absence of a specified body of water, the discharge is removed from the model.

#### *MODEL CONSTRUCTION AND CALIBRATION*

The model represents a conceptualization of the study area, encompassing a  $\sim 1 \text{ km}^2$  area divided into 30m square grid cells. F6, an outlying wellsite in the study area, is excluded from the model to avoid extrapolating head and land surface elevation data over hundreds of meters and consequently increasing the likelihood of high error [Figure 6a]. Variable unsaturated thickness is modeled using DEM surface elevation data and water table data interpolated over the entire model area [Figure 6b].

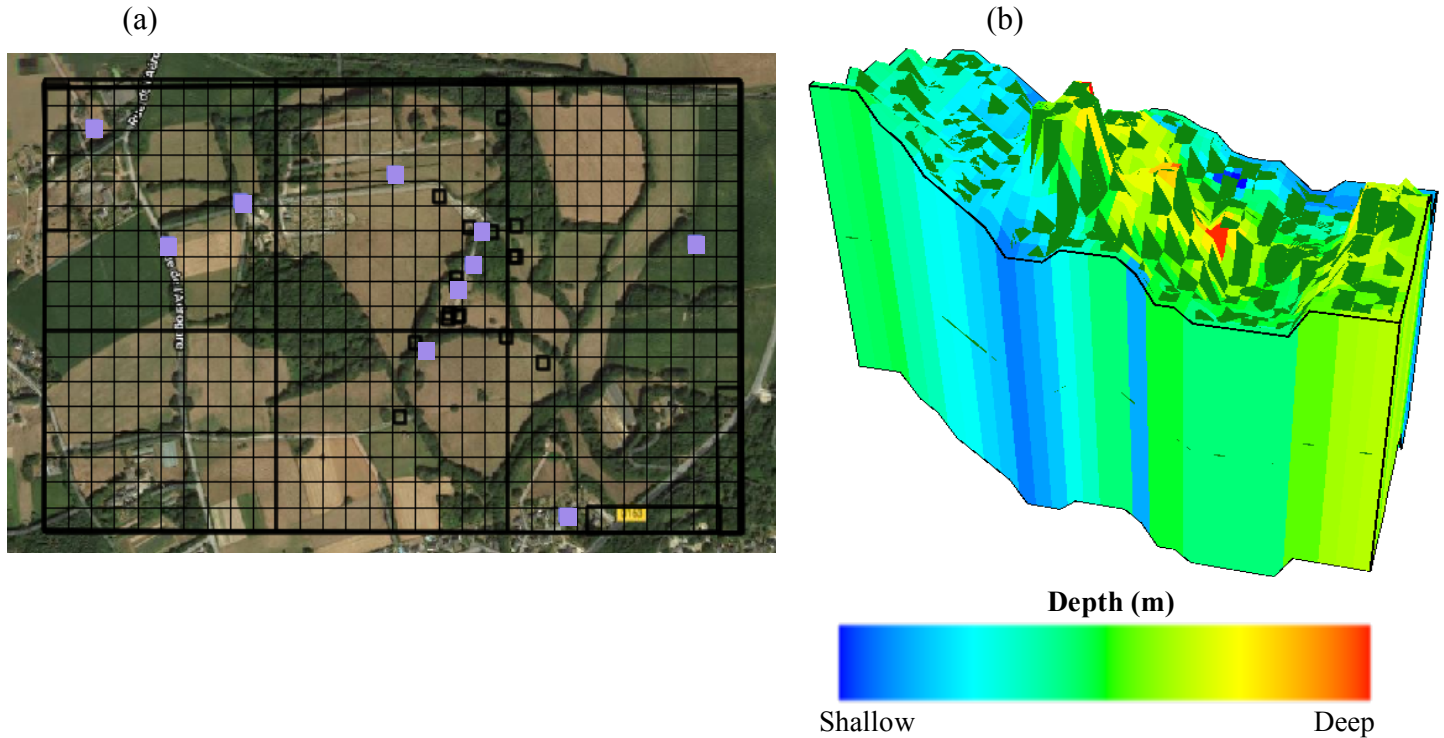


**Figure 6:** (a) Plan view of model, showing gridded area and well locations geo-coded over a GoogleEarth satellite image of Ploemeur; model is oriented north, with purple squares indicating wells used in this study (b) 3-D render of model, colored to show thickness of vadose zone

Hydraulic head averages for each of ten wells are calculated from daily measurements made at the H+ hydrogeologic site; the oldest wells have been monitored since 1991, whereas the newest well's measurements date back to 2006. Head averages are calculated and modeled for each month in order for entry into the CHD package in MODFLOW. Entries are made for each of 12 stress periods, and are repeated for subsequent modeled 'years'. The Preconditioned Conjugate Gradient (PCG) solver is used when running the models, with head and residual closures of 0.001 and a relaxation parameter of 1.

The infiltration rate and evapotranspiration demand data are averages calculated from over 25 years of daily measurements (**Table 1**). Infiltration is the downward rate of

water movement expressed as units of length per time at the modeled land surface for each cell column; the rates must be less than the vertical hydraulic conductivity to avoid being set equal to the latter variable (*Winston, R.B., 2009*).

Starting Time (d)	Ending Time (d)	Infiltration Rate (m/d)	ET Demand (m/d)
0	31	0.00346	0.00065
31	59	0.00268	0.00092
59	90	0.00206	0.00152
90	120	0.00226	0.00228
120	151	0.00209	0.00296
151	181	0.00164	0.00362
181	212	0.00183	0.00367
212	243	0.00171	0.00323
243	273	0.00187	0.00244
273	304	0.00314	0.00136
304	334	0.00343	0.00084
334	365	0.00332	0.00071

**Table 1.:** Showing the input values for the Unsaturated Zone Flow package as they were entered for one year of run time; this is just a sample, considering that these values were re-entered for each subsequent year of run time.

Infiltration is applied in relation to the specified water content of the model when the flux is assumed to be equal to the unsaturated hydraulic conductivity; this process is to apply the characteristic solution method for unsaturated flow, and is outlined in Charbeneau's equation (*1984; Niswonger et al., 2006*):

$$\theta = \left(\frac{q_{in}}{K_s}\right)^{\frac{1}{\varepsilon}} (S_y) + \theta_r \quad 0 < q_{in} \leq K_s \quad (11a)$$

$$\theta = \theta_s \quad K_s < q_{in} \quad (11b)$$

where

$\theta$  is the water content of an infiltration wave

$q_{in}$  is the infiltration rate

$\epsilon$  is the Brooks-Corey exponent

$K_s$  is the saturated hydraulic conductivity

$S_y$  is specific yield

$\theta_r$  is residual water content

$\theta_s$  is saturated water content

The evapotranspiration demand is the rate of ET in each column of cells that falls within the extinction depth interval, which is the depth below the surface elevation beyond which ET does not occur. Related to these processes is the ET extinction water content, a value of water content below which ET is unable to be removed from the unsaturated zone (Niswonger *et al.*, 2006; Winston, 2009). Both extinction depth and water content have been established in previous studies, and are listed as 3 m below land surface and 0.13, respectively (Leray *et al.*, 2012; Jimenez *et al.*, 2013).

A series of parameter adjustments was designed to recreate reasonably similar recharge estimates compared to those published in Jimenez *et al.* (2013) as a baseline. Jimenez-Martinez and his team calculated an estimated aquifer recharge of 169-282 mm at the Ploemur site by using soil storage volume, estimated from soil thickness and field capacity, for the years 2003-2010; however, they specifically excluded unsaturated zone processes in their calculations, hence the reason their results were utilized in this project as a preliminary baseline for an investigation into the effect of vadose thickness and not as an explicit calibration value.

The UZF1 package uses the difference between the land surface and the water-level elevation as the unsaturated zone thickness. The bottom of the model is designated 40 m



below the land surface, as this is generally the extent of the regolith thickness at the study site (*Leray et al., 2012*). General head boundaries are implemented in the northwest and southeast sections of the model, consistent with flow direction at the site. The model is represented as containing 12 monthly stress periods and a total of 365 daily time steps, running for one year at a time under transient conditions and repeating until steady state is achieved in order to allow the user to observe the seasonal trends present at the site and examine the factors contributing to those changes in recharge. Input values for infiltration and evapotranspiration demand are allowed to vary for different tests of the model, and include individual monthly averages for the last several years (2009 - 2015), individual monthly averages for the years that Jimenez and his team completed their calculations (2003 – 2010), and finally running the repeating monthly values averaged over the entire 25-year dataset.

#### *STATISTICAL ANALYSIS USING MATLAB*

A statistical analysis of the hydrogeologic data is conducted and involves writing a variety of MATLAB scripts that performed complex functions on twenty-five years of data. Initial data manipulation involves calculating the average daily precipitation, ET, and head values for each month of the year using records provided by the Ploemeur H+ hydrologic observatory (*Jimenez et al., 2013*). While precipitation and evapotranspiration have been consistently measured at daily intervals from 1991-present, head measurements from the ten observation wells used in this study were primarily taken at daily intervals but have varied start dates. Contour maps of the averaged head values from the sample of

observation wells are generated to provide a comprehensive visual of the water table elevation over the extent of the study area [Figure 7].

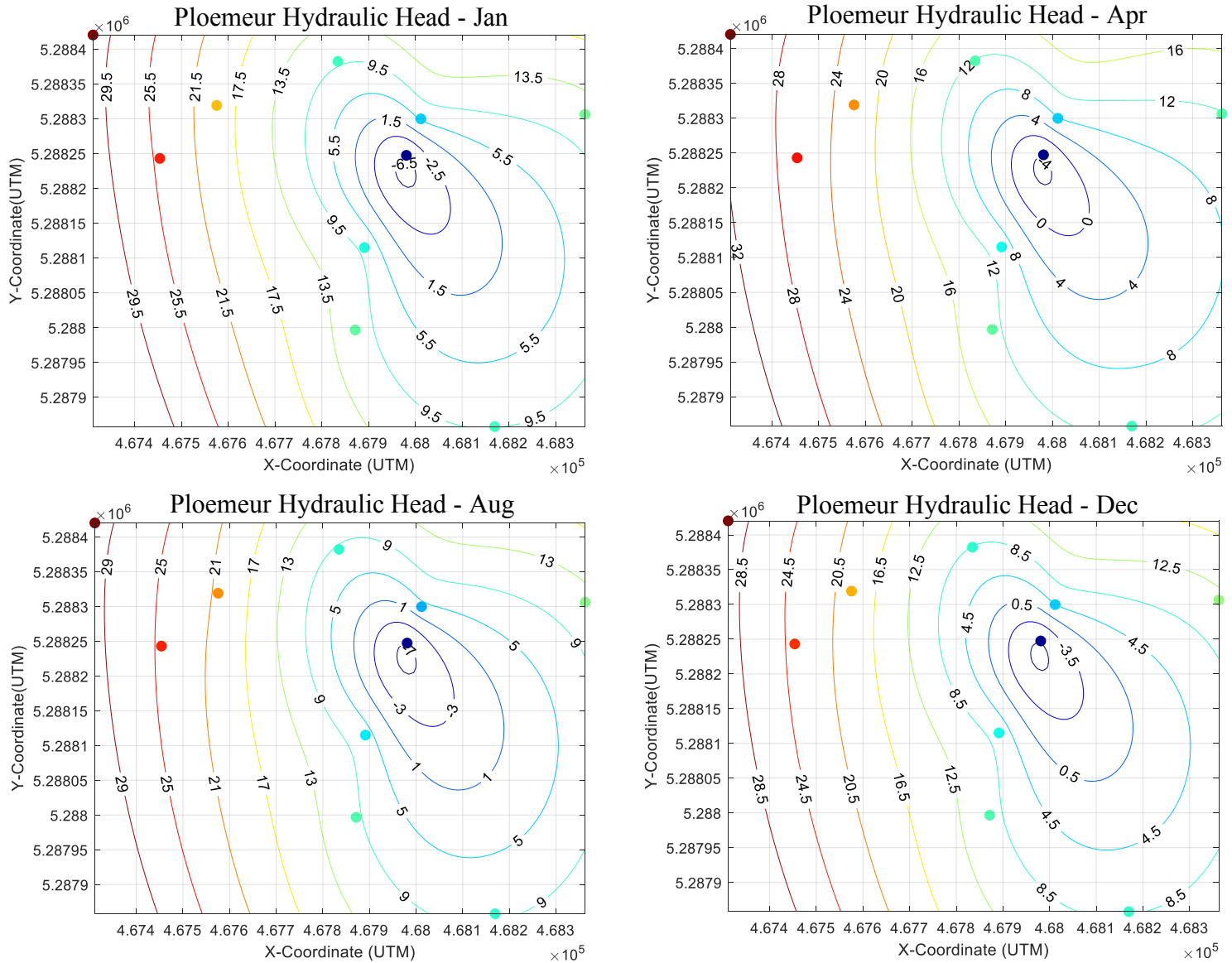


**Figure 7:** Displaying the average daily hydraulic head values at intervals during the calendar year. Plots were created using the contour function for gridded data in MATLAB R2018b. Negative values indicate areas where head has fallen below sea level. Wellsites are depicted as filled circles with colors corresponding to the nearest head level contour, and contour values are in meters.

In the contouring process, p-chip interpolation is used to estimate the water level measurements at daily intervals, in order to create data sets of consistent size that can be

used in time-saving bulk commands. The p-chip interpolated data sets display a mean-squared error of only 0.3427 compared to the raw data.

Further analysis involves constructing a three-dimensional rendering of the site [Figure 8] showing the spatial variability in the vadose thickness.

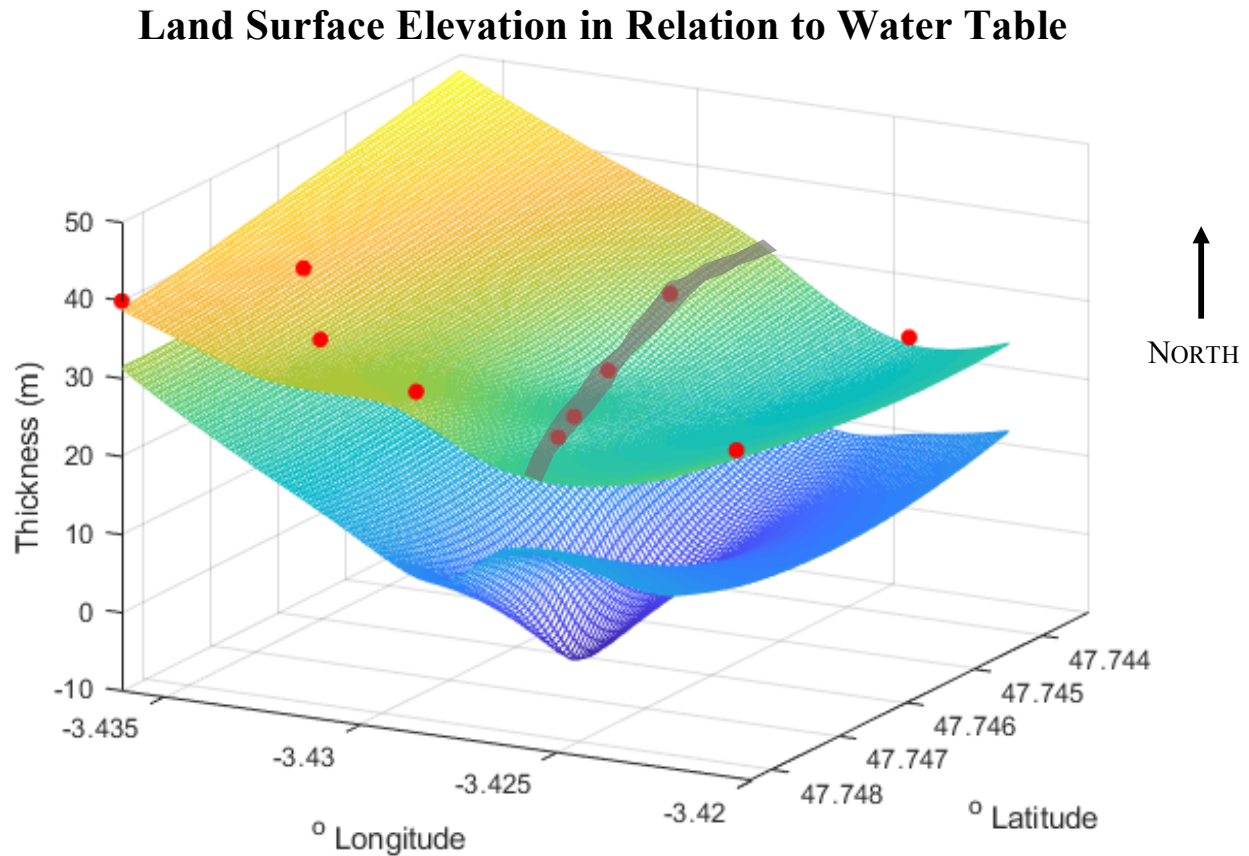


**Figure 8:** A mathematical conceptualization of the study site, with the top plane showing the changes in topography and the bottom showing the changes in water table elevation interpolated from hydraulic head measurements; a slight cone of depression can be observed surrounding the pumping location. For orientation purposes, the fault location is roughly represented in gray. Wellsites used in this study are depicted in red. Note: y-axis is inverted.

The plane of the land surface elevation data is plotted atop a plane of the water table data in a 3-dimensional scatter plot with a 101-node grid, created using the ‘mesh’ and

‘griddata’ commands in MATLAB; the vadose zone is represented by the negative space between the two planes. All coordinate points were originally recorded in Lambert II Centre, as this coordinate system is more common in France where the data are recorded; they are converted to decimal latitude and longitude degrees for ease of understanding in this study.

Post-model analysis examines the different distributions of the UZF model outputs [Figure 9] for the various dataset tests using the cumulative volumetric budget values from the MODFLOW list file. Cumulative values for infiltration, UZF ET, and UZF recharge from the end of each monthly stress period are used and shown in [Figure 10].

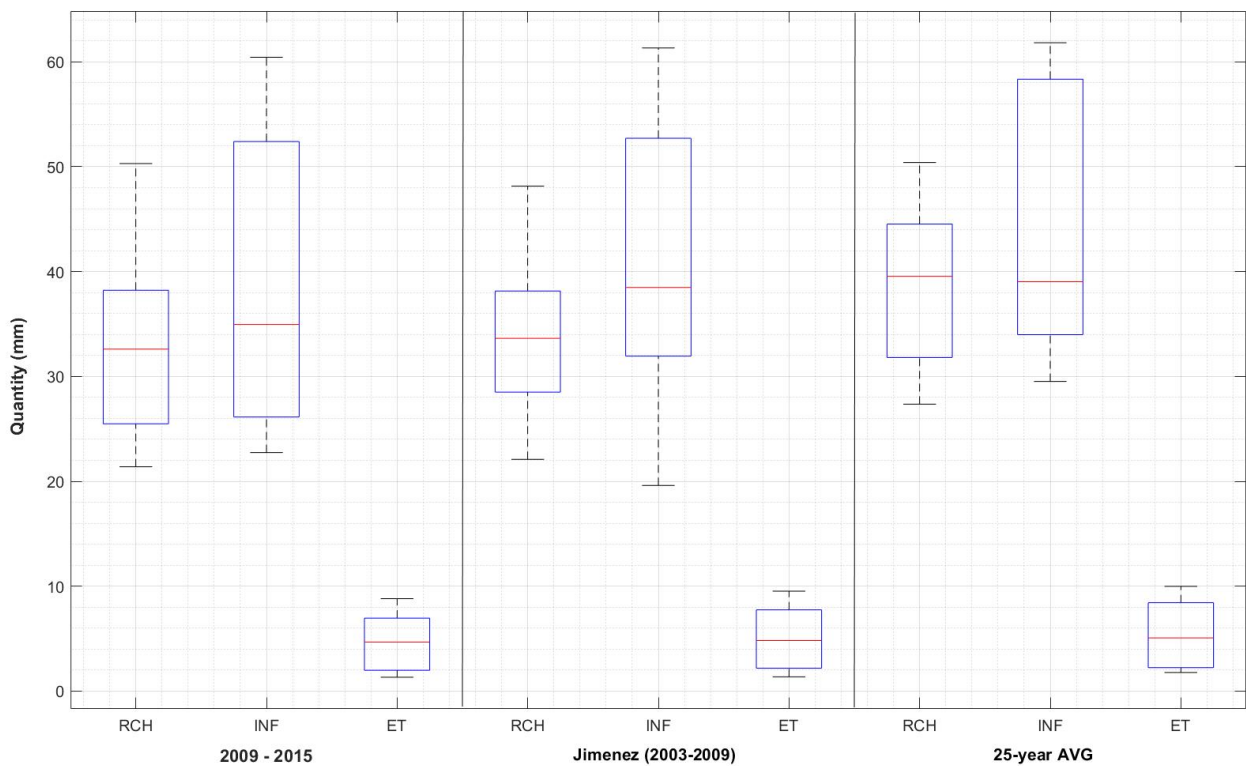


**Figure 9:** Distributions of the three tests run using the quantification model, showing differences in mean and spread between the datasets.

CUMULATIVE VOLUMES	L**3	RATES FOR THIS TIME STEP	L**3/T
<hr/>			
IN:		IN:	
---		---	
INFILTRATION =	1235638.3265	INFILTRATION =	1524.5439
OUT:		OUT:	
---		---	
UZF ET =	441992.8679	UZF ET =	143.0425
UZF RECHARGE =	719700.4185	UZF RECHARGE =	714.8217
IN - OUT =	73945.0401	IN - OUT =	666.6797
STORAGE:		STORAGE:	
-----		-----	
STORAGE CHANGE =	73944.3353	STORAGE CHANGE =	666.6798
PERCENT DISCREPANCY IS DIFFERENCE BETWEEN IN-OUT MINUS CHANGE IN STORAGE DIVIDED BY THE AVERAGE OF IN AND OUT TIMES 100			
PERCENT DISCREPANCY =	0.00	PERCENT DISCREPANCY =	0.00

**Figure 10:** Highlighting the values from the model output used in calculating the monthly sums of infiltration, recharge, and ET.

The budget values for a particular month are subtracted from each subsequent stress period and divided by the total study area, shown in **Eq. 12a & 12b**, to determine the monthly quantities of infiltration, UZF ET, and UZF recharge in meters:

$$\frac{(\text{RCH at final time step in stress period N}) - (\text{RCH at final time step in stress period N-1})}{\text{Area of model}} = \text{Monthly RCH} \quad (12a)$$

$$(719,700 \text{ m}^3 - 699,474 \text{ m}^3) / 859,871 \text{ m}^2 = 0.0235 \text{ m} \quad (12b)$$

A sensitivity analysis of the UZF input parameters involves using the 25-year averages model outputs. Each of six parameters are altered between -15% and +15% from baseline value to determine the perturbation effects on the UZF outputs. These parameters are: initial unsaturated water content, saturated water content, maximum unsaturated vertical conductivity, residual water content, extinction content, and extinction depth. The cumulative values produced from the model runs with altered parameters are examined at each of 12 stress periods during a modeled year and compared to the baseline values from the original model. Independence between model inputs is assumed.

## **Results & Discussion**

### *VADOSE ZONE THICKNESS & TEMPORAL RECHARGE DISTRIBUTION*

Model results show that variations in vadose zone thickness do have a measurable effect on the lag time observed between precipitation events and the subsequent observed changes in the water levels at the Ploemeur site. Figure 11 shows the simulated temporal distribution of cumulative volumetric recharge in model cells of varying thickness, in comparison to the cumulative volumetric infiltration. If the vadose zone had no effect on travel time, the infiltration and recharge data would be indistinguishable. However, the plotted results from the UZF simulations clearly show the effect that vadose thickness has on recharge arrival time, and therefore the influence that vadose thickness exerts over the lag time at this site.

A positive linear relationship between vadose thickness and lag time appears to exist until the thickness of the unsaturated zone exceeds 20 m. At unsaturated depths > 20 m the direct relationship appears to reverse, as cells modeled with increasingly thick vadose zones appear to receive recharge more rapidly than some of their thinner counterparts (**Table 2**). The lag time between infiltration and recharge during one year as determined from this model is 104 days, as calculated based a spatially averaged vadose thickness from cell-by-cell water table results [Figure 12] and temporally averaged cumulative volumetric recharge quantity. The lag from the empirical precipitation and hydraulic head data shows an average 142-day lag, meaning that 73% of the observed lag can be explained by vadose zone processes.

## Effect of Variable Vadose Thickness on Recharge Time

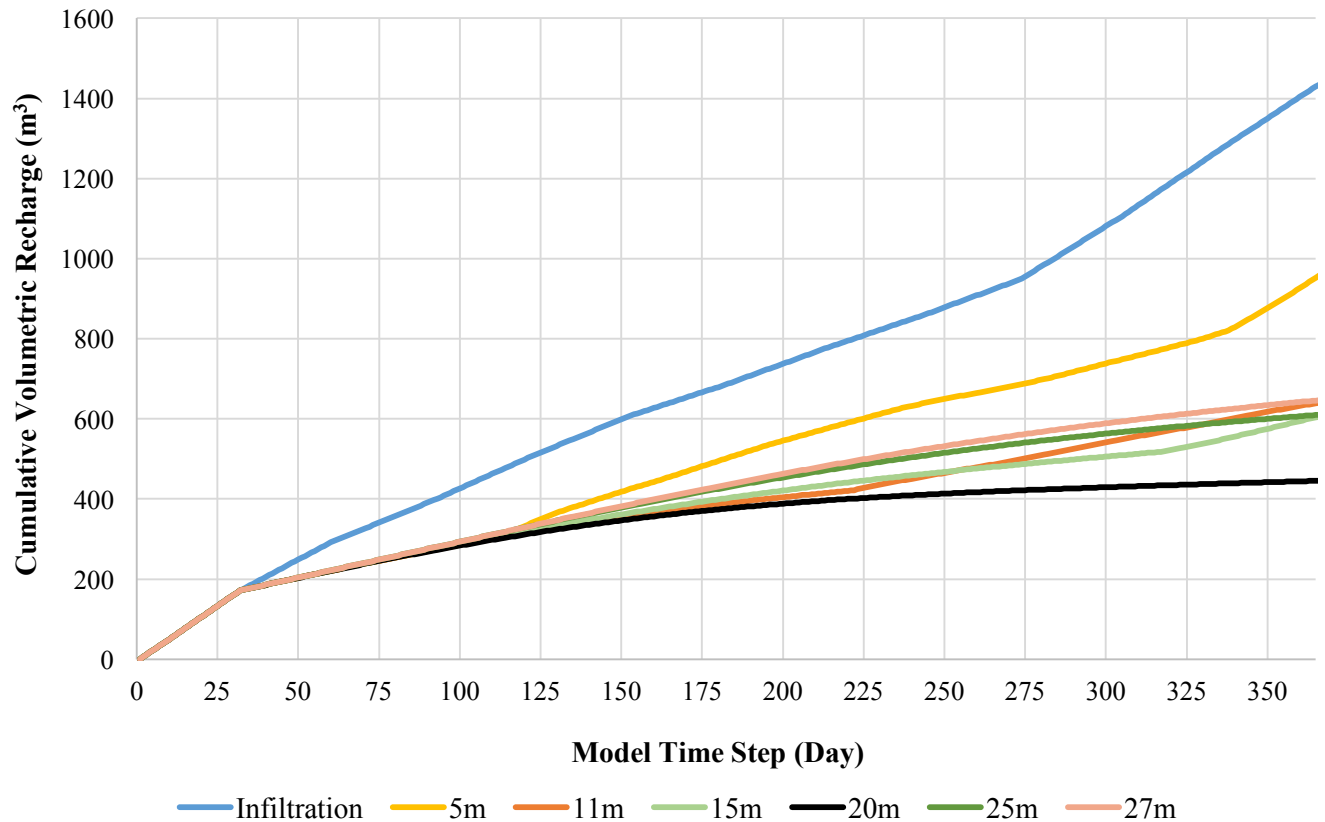


**Figure 11.:** The effect of varying unsaturated zone thickness on recharge quantity. The baseline, infiltration, is analogous to zero vadose thickness and is represented as the top line in blue. Subsequent thicknesses, varying in ~5m intervals before showing the maximum thickness, are symbolized by the designated lines below and show that Vadose thickness affects the time it takes for a given amount of infiltration to be reflected in the groundwater reservoir as recharge. The model simulates one year of data, in daily time steps.

A similar linear trend between unsaturated zone thickness and delay in water-level response time is observed in the Chalk aquifer in England, where the time lag appears to correlate strongly to the thickness of the vadose zone. Four sites at this English aquifer that had the largest unsaturated zone thicknesses showed a significant increase in lag time at and below a critical vadose thickness. Another likeness is observed in the changes in slope



of the response time vs. thickness plotlines, indicative of potential changes in dominant flow pathways (i.e. matric flow to fracture/fissure flow) (Lee et al., 2006).

Infiltration Timestep at 500 m <sup>3</sup> : 120			
Vadose Thickness	Timestep at 500m <sup>3</sup>	Vadose Thickness	Timestep at 500m <sup>3</sup>
5 m	181	20 m	751
11 m	274	25 m	236
15 m	291	27 m	225

**Table 2:** Lengths of modeled time necessary for UZF recharge to attain a given cumulative quantity in cells with each of the plotted thicknesses, compared to the amount of time steps necessary for cumulative infiltration to reach that same quantity.

This non-linear trend is likely influenced by the changing monthly head values that are used in the modeling procedure and shown in Figure 7; certain head levels are tied to each stress period, necessitating a certain sum of recharge to move through the system and influence those head levels. The non-linearity observed in the thicker vadose sections is therefore influenced by the amount of hydraulic head change that occurs in those wells located in a thicker part of the vadose zone. Wells with hydraulic heads that exhibit larger fluctuations throughout the year necessitate larger influxes of recharge, despite the depth at which they are located.

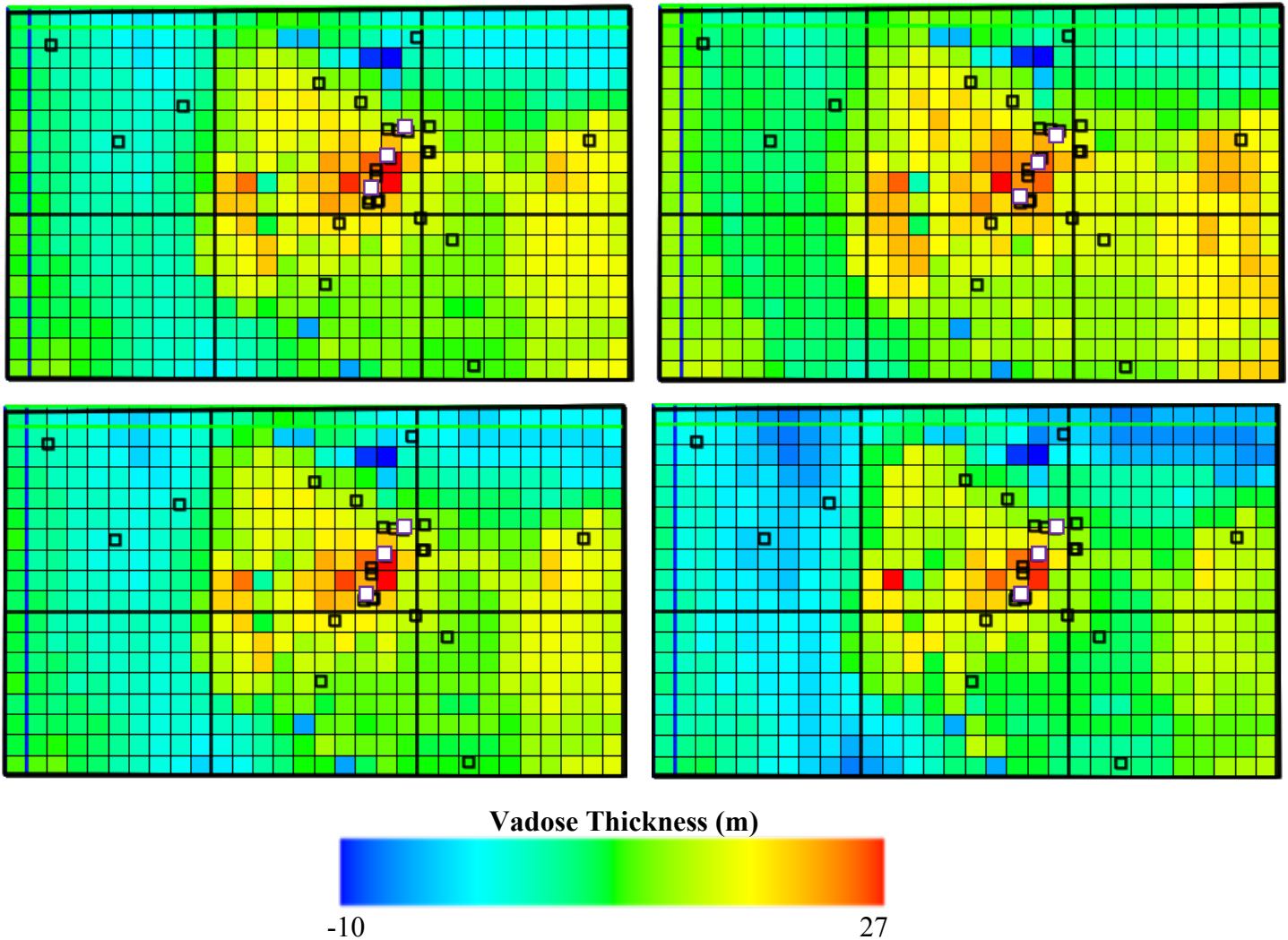


*Figure 12.: Vadose thickness in January, April, August, and December (clockwise from upper left:). Deepest blue values represent the small cluster of negative thickness values. The thickest portions of the unsaturated zone consistently remain clustered at the pumping site within the fractured fault zone, where a cone of depression has formed after nearly three decades of highly productive withdrawals. Black squares represent wellsites; white squares lined in purple are pumping wells.*

The fact that this non-linear relationship exists suggests that while a significant portion of the lag time observed at the site can be attributed to the vadose zone thickness, this is not the only parameter affecting the downward movement of water through the

unsaturated zone, and further investigation into the nuances of the fractures and structures at the site is necessary to fully account for the entire observed lag. This is further corroborated by the simulated vadose thickness. The negative vadose thickness modeled in these few cells is not explained by the properties of the vadose zone, but rather points to preferential flow paths in areas that allow meteoric water to move more quickly through the unsaturated zone and provide recharge to the groundwater system.

#### *SPATIAL DISTRIBUTION OF RECHARGE*

Simulated monthly recharge is the greatest [Figure 13] in the western part of the region--west of the fault zone, and lowest within the fault zone and regions to the east where the drawdown is generally the greatest. Enhanced recharge is also observed along the western and northern boundaries of the model where elevations reach upwards of 40m above sea level compared to the ~20m towards the fault zone and center of the model, and where hydraulic heads have historically been significantly higher than those recorded in wells near the pumping zone. The recharge patterns below reflect the combination of head contours entered during model construction, the modeled topography, and the simulated vadose thickness. Areas with the greatest depth between the model surface and the calculated water table display minimal recharge, while areas with shallower unsaturated zones tend to exhibit higher rates per month.

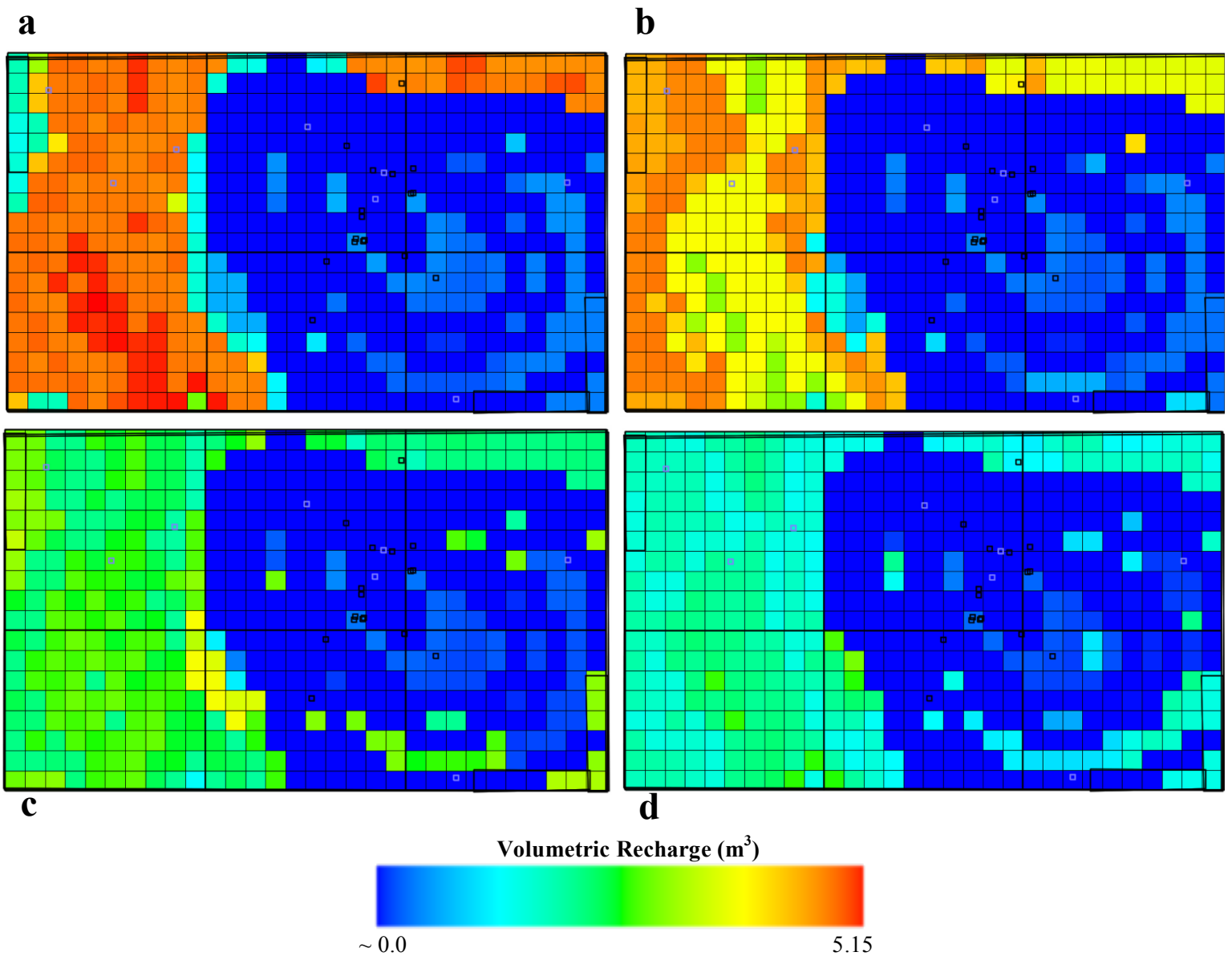


**Figure 13.:** The spatial distribution of recharge, showing that topographically higher areas and cells with thinner unsaturated zones tend to be simulated with more UZF recharge. (a) January recharge (peak infiltration); (b) March recharge (peak recharge); (c) June recharge (minimum infiltration); (d) September recharge (minimum recharge). Rectangles show locations of wells.

#### SEASONAL RECHARGE QUANTIFICATION

Simulated temporal recharge reveals that much of the lag in recharge response can be attributed to vadose zone properties and processes. A similar trend, akin to a sinusoidal

curve, can be observed between the UZF-modeled recharge [Figure 14] and the measured head data at the study site provided earlier in this paper in Figure 2.

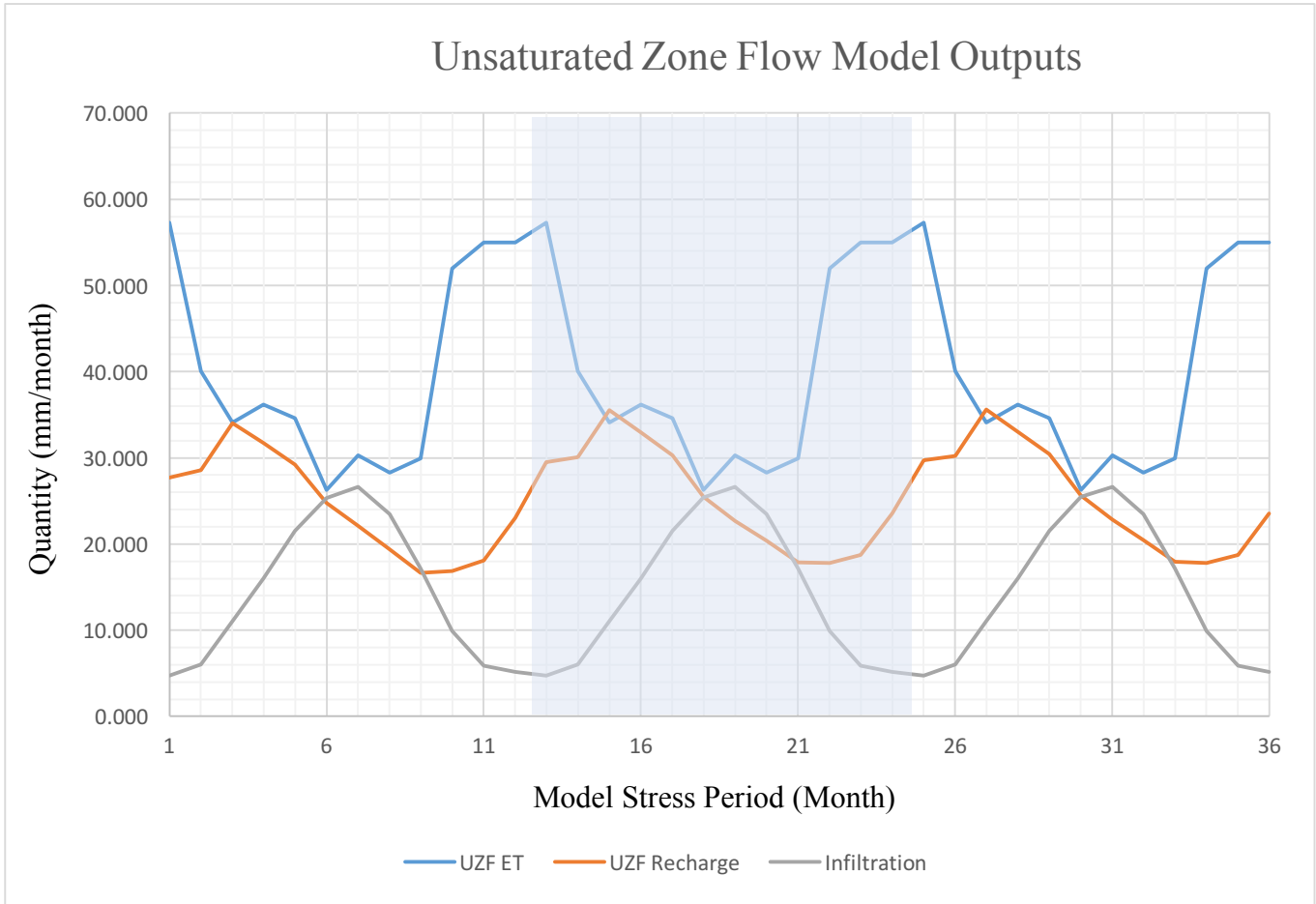


**Figure 14.:** Simulated measurements of infiltration, UZF recharge, and UZF ET quantities (blue, orange, and gray, respectively), revealing consistent seasonal distribution trends in each of the three components over the 36-month simulation period. The shaded portion serves to identify the boundaries between modeled years 1 & 2 (left edge) and modeled years 2 & 3 (right edge). ET and infiltration curves exhibit inverse trends, with the former peaking in the summer months (6-8) and the latter peaking in the winter months (11-12, 1) of each modeled year. The recharge curve shows a maximum occurring in the third month of each simulated year, 2-3 months after the maximum infiltration occurrence.

The recharge signal derived from the UZF model exhibits an average 2 months of lag between peak infiltration, which occurs between December-January, and the resulting

peak recharge that typically occurs between March and April. This temporal recharge pattern is nearly identical to the 2-3 month average lag observed in the empirical precipitation and hydraulic head data. This provides compelling evidence for the results from the first part of this investigation stating that the vadose zone is an essential factor in the delay observed between the precipitation event (infiltration) and the water levels measured in the wells at the site.

It is worth noting that recharge is simulated to occur during each month of the year, despite the increase in evapotranspiration demand that occurs in the area during the summer months when ET can exceed total precipitation. Water loss by ET is greater than infiltration between April and September, leading to a decrease in the average hydraulic heads between May and October/November [Figure 15].

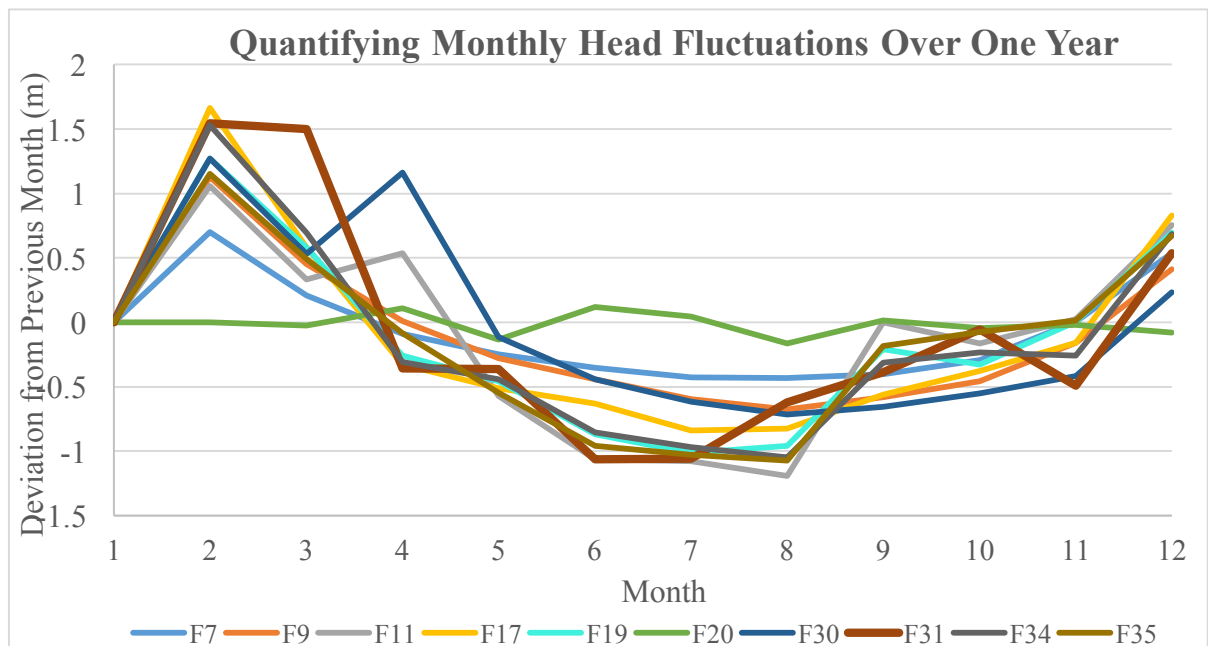


**Figure 15.:** Plot showing the amount of simulated head change in 10 of the observation wells at Ploemeur. Most wells exhibit a decrease in head during the summer and autumn months; well 20 is notably contrary to this pattern, exhibiting an increase in head during June, July, and September.

The relationship between infiltration and evapotranspiration in the UZF package is calculated using empirically derived values from prior studies for the extinction depth, extinction content, and vertical hydraulic conductivity, and the amount of ET simulated depends heavily on the initial water content derived through parameter estimation and model calibration [Figure 16]. The calculation of distributed recharge occurring throughout the calendar year is novel for this site. Previous investigations, based on the simplified conceptualization of Infiltration – Evapotranspiration = Recharge, led to the assumption that no recharge could occur at the water table without water actively entering the subsurface as infiltration; however, the overwhelming majority of preceding studies did not explicitly model vadose zone properties and processes, much less areas with more robust unsaturated zones within fractured crystalline rock spanning tens of meters.

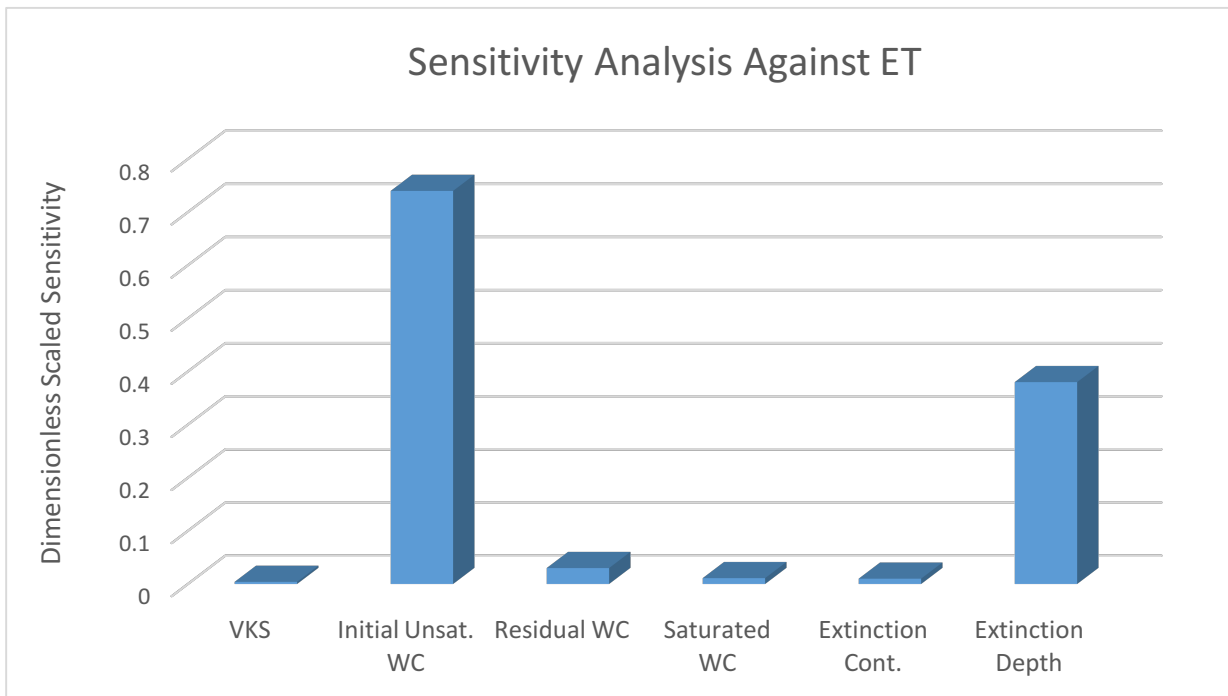


**Figure 16.:** Sensitivity of input parameters in relation to evapotranspiration simulation, supporting that initial unsaturated water content, extinction depth, and residual water content are the strongest constraints specifically related to evapotranspiration quantity.

Conversely, we are showing that under certain conditions it is possible for a system to continue to receive recharge even when evapotranspiration demand exceeds the precipitation within a given time period. Typically, water would be removed from the simulated water table in a model when ET demand exceeds infiltration; however, this site contains a relatively deep water table coupled with a comparatively shallow extinction depth, and a relatively large vertical saturated conductivity (VKS) that allows water to travel through the subsurface more quickly than can be utilized by plants, adding to the unique recharge distribution observed at the site.

A similar recharge signal was recorded during a study by Rodhe et al. (2004), conducted on a fractured crystalline rock aquifer in Sweden. In this instance, results showed recharge occurring during each month of the year and supported the initial hypothesis that the aquifer was supplemented by vertical recharge from groundwater in the overlying soil layer. While the recharge at this site was significantly less than that of Ploemeur, estimated at only  $\sim 20 \text{ mm yr}^{-1}$ , the similarity in the signals lends support to our model results.

Table 3 summarizes the monthly quantity of infiltration, UZF recharge, and UZF ET. All values are converted to millimeters for ease of comparison to previous studies. The results of this investigation indicate that the simulated annual quantity of recharge ranges from 304-307 mm. In comparison, calculations by Jimenez et al. in 2013 predicted recharge between 169 mm – 282 mm per year, a range significantly lower than that produced by model simulations in this investigation. It should be noted too that the entire annual recharge in the Jimenez et al. (2013) investigation typically occurs over a three- to four-month period during the winter months.



The differences between the results of this study and those published in Jimenez et al. (2013) stem from a number of factors, including consideration of heterogeneity and vertical flow representation. Jimenez and his team used recharge at the bottom of the soil layer as input in their calculations specifically to reduce non-linearity from the vadose zone, whereas our model examines vadose zone processes such as wetting plane mobility and the subsequent influence on the infiltration quantities.

Month	Monthly Infiltration (mm)	Monthly Recharge (mm)	Monthly ET (mm)	Month	Monthly Infiltration (mm)	Monthly Recharge (mm)	Monthly ET (mm)	Month	Monthly Infiltration (mm)	Monthly Recharge (mm)	Monthly ET (mm)
1	57.280	27.683	4.720	13	57.280	29.500	4.721	25	57.280	29.730	4.721
2	40.074	28.589	6.035	14	40.074	30.103	6.035	26	40.074	30.252	6.036
3	34.103	33.998	11.039	15	34.103	35.499	11.040	27	34.103	35.608	11.040
4	36.207	31.762	16.024	16	36.207	32.940	16.025	28	36.207	33.055	16.026
5	34.600	29.182	21.497	17	34.600	30.296	21.498	29	34.600	30.416	21.500
6	26.274	24.752	25.355	18	26.274	25.484	25.444	30	26.274	25.618	25.446
7	30.296	22.088	26.651	19	30.296	22.692	26.655	31	30.296	22.803	26.657
8	28.309	19.409	23.446	20	28.309	20.354	23.460	32	28.309	20.425	23.462
9	29.959	16.641	17.132	21	29.959	17.906	17.150	33	29.959	17.952	17.152
10	51.983	16.849	9.873	22	51.983	17.785	9.878	34	51.983	17.826	9.879
11	54.952	18.109	5.902	23	54.952	18.718	5.904	35	54.952	18.741	5.905
12	54.963	23.041	5.156	24	54.963	23.522	5.157	36	54.963	23.538	5.15

**Table 3.:** Graph showing the total monthly simulated quantities for the indicated UZF parameters over the 36 months of simulation time, which is equivalent to 36 stress periods containing 365 time steps each.

Transit time between infiltration and recharge was previously considered to be instantaneous and lag time was attributed to slow-moving water percolation through the low-permeability mica-schist into the contact zone, thus leading to the calculated differences in recharge between these two studies. Additionally, the 2013 investigation employed water level datasets from different wells at the site than those used in this study

[Figure 17]. It's also possible that the size of the model domain could exert a moderate influence on recharge estimates and the domain area used in the Jimenez-Martinez's study was slightly smaller than the  $\sim 1 \text{ km}^2$  domain used in this investigation.

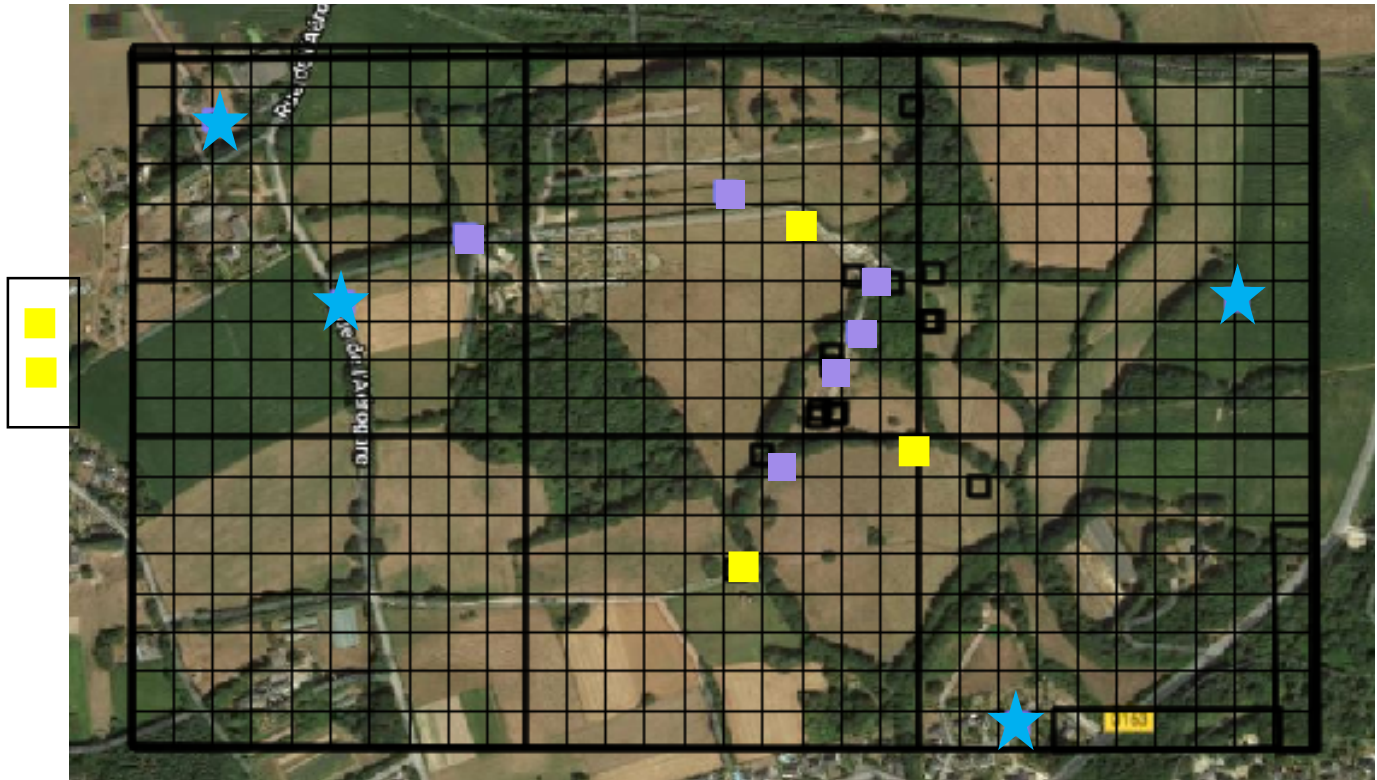


**Figure 17.:** Locations of the wellsites used exclusively for this study (purple squares), the wellsites used exclusively in the investigation conducted by Jimenez et al., 2013 (yellow squares), and wellsites used in both studies (blue stars). The two yellow squares to the site represent wellsites used in the 2013 study that are located at an adjacent site  $\sim 3$  kilometers west of Ploemeur. Black square outlines symbolize wells not used in either study.

Interpolation methods vary between the studies as well; the aforementioned study used linear interpolation for gaps in their piezometric head datasets, whereas, as outlined in the Methods section of this paper, gaps in the head data (generally only a few days at most), are interpolated from both raw datasets and p-chip interpolation (with a very low error of 0.3% between the two methods). Finally, the initial estimation of the Ploemeur recharge

signal in the previous investigation was calculated using hydraulic head values from years 2003-2010, whereas this study uses a more extensive hydraulic head dataset dating back to 1991 and extending to 2015.

#### *UNCERTAINTY*

Sources of uncertainty in the model stem from various sources, including parameter value approximations and inherent assumptions. Parameters at the Ploemeur site such as vertical hydraulic conductivity, Brooks-Corey coefficient, and residual water content were approximated with some initial, shallow investigations but were not examined thoroughly within the fractured rock. The UZF modeling package relies on some inherent assumptions, including uniform hydraulic properties within the vadose zone and unsaturated flow that is driven solely by gravimetric potentials. Additionally, uncertainty arises from the lack of structure specified in this model, as fracture flow and preferential flow paths are not specifically accounted for in the hydraulic head gradients and recharge distribution.

## **Conclusions**

Characterizing fractured rock aquifers remains a challenging issue for groundwater modelers, as heterogeneous materials and subsurface structures add complexity to the system. Understanding such systems is crucial to the effective and sustainable management of groundwater resources as these reservoirs continue to be exploited.

The fractured rock aquifer system in Ploemeur, France, is investigated to better understand the properties and processes constraining a unique recharge signal within a highly productive groundwater reservoir that shows a lag of approximately two months between seasonal precipitation trends and subsequent effect on measured water levels in the crystalline rock aquifer. A model was constructed using MODFLOW-2005 with ModelMuse as the GUI; the Unsaturated Zone Flow and Time-Variant Specified Head packages were used, alongside the Pre-conditioned Conjugate Gradient solver, to simulate the movement of water through the unsaturated zone within this crystalline aquifer complex. The goals of this model were to determine the extent to which vadose zone thickness and vertical hydraulic conductivity of the vadose zone affected the timing of recharge to the underlying crystalline-rock aquifer, and to quantify the average seasonal recharge trends at the site.

Twelve stress periods totaling 365 time steps were used to represent the days of the year. These stress periods were repeated for successive years to ensure consistency in results and mimic yearly variations in precipitation and ET. Constant input parameters for the unsaturated zone included the Brooks-Corey epsilon value, residual water content, initial unsaturated water content, saturated water content, VKS, extinction depth and

extinction water content. MATLAB was used to calculate average infiltration rates, evapotranspiration demands, and head values over each stress period.

Results show that vadose thickness does have a tangible effect on recharge lag time, albeit a non-linear one. Once vadose zone thickness exceeds 20m recharge lag time begins to decrease, which suggests that further investigation into the subsurface structure and preferential flow paths therein is necessary to fully explain the groundwater movement at Ploemur beyond the 73% of lag time accounted for by the vadose zone. Seasonal trends in recharge show a very similar trend to head values at the site, which exhibit peak values occurring in March and minimum values occurring in September. Most notable is the fact that this model simulates recharge to the underlying aquifer during each month of the year, which is vastly different than previous investigations what suggest recharge occurs only during the winter months when ET is low.

## References

- Abbott, M.B. (1966). An Introduction to the Method of Characteristics. *American Elseviers*, New York.
- Ali, M. (2017). Quantifying Natural Groundwater Recharge Using Tracer and Other Techniques. *Asian Journal of Environment & Ecology*. 5. 1-12. 10.9734/AJEE/2017/36811.
- Amiotte-Suchet, P., Probst, J.L., & Ludwig, W.(2003). Worldwide distribution of continental rock lithology: implications for the atmospheric/soil CO<sub>2</sub> uptake by continental weathering and alkalinity river transport to the oceans. *Global Biogeochemical Cycles* 17, 1038.
- Aquilina, L., Roques, C., Boisson, A., Vergnaud-Ayraud, V., Labasque, T., Pauwels, H., Bour, O. (2018). Autotrophic denitrification supported by biotite dissolution in crystalline aquifers (1): New insights from short-term batch experiments. *Science of the Total Environment*, 619–620, 842–853.
- Aquilina, L., Vergnaud-Ayraud, V., Les Landes, A.A., Pauwels, H., Davy, P., Pételet-Giraud, E., Labasque, T., Roques, C., Chatton, E., Bour, O., BenMaamar, S., Dufresne, A., Khaska, M., La Salle, C.L.G., Barbecot, F. (2015). Impact of climate changes during the last 5 million years on groundwater in basement aquifers. *Scientific Reports* 5, 14132.
- Baalousha, H. (2009). Fundamentals of Groundwater Modelling. *Groundwater: Modelling, Management and Contamination*, (January 2011), 113–130.
- Bense, V. F., Gleeson, T., Loveless, S. E., Bour, O., & Scibek, J. (2013). Earth-Science Reviews Fault zone hydrogeology. *Earth Science Reviews*, 127, 171–192. <https://doi.org/10.1016/j.earscirev.2013.09.008>
- Berkowitz, Brian. (2002). Characterizing flow and transport in fractured geological media: A review. *Advances in Water Resources*. 25. 861-884.
- Blatt, H. and Jones, R.L (1975). Proportions of exposed igneous, metamorphic, and sedimentary rocks. *Geol. Soc. Am. Bul.* 86, 1085-1088.
- Bouwer, H. (1978) *Groundwater Hydrology*. McGraw-Hill, New York

- Buttle, J.M. & Sami, K. (1990). Recharge Processes During Snowmelt: An Isotopic and Hydrometric Investigation. *Hydrological Processes*. 4. 343 - 360.
- Charbeneau, R.J., 1984, Kinematic models for soil moisture and solute transport: *Water Resources Research*, v. 20, no. 6, p. 699-706.
- Cassiani, M., Radicchi, A., Albertson, J.D., Giostra, U., 2007. An efficient algorithm for scalar PDF modelling in incompressible turbulent flow; numerical analysis with evaluation of IEM and IECM micro-mixing models. *Journal of Computational Physics*, **223**, 519-550.
- Childs, E.C. & Collis-George, N. (1950). The Permeability of Porous Materials. Proceedings of the Royal Society of London. *Series A, Mathematical and Physical Sciences*. 201. 392-405.
- Crosbie, R. S., Binning, P., & Kalma, J. D. (2005). A time series approach to inferring groundwater recharge using the water table fluctuation method, *41*, 1–9. <https://doi.org/10.1029/2004WR003077>
- Darcy, H. (1856). *Les Fontaines Publiques de la Ville de Dijon*. Dalmont, Paris. 647 p
- Dewandel, Benoit & Maréchal, Jean-Christophe & Bour, Olivier & Ladouche, Bernard & Ahmed, Shakeel & Chandra, Subash & Pauwels, Hélène. (2012). Upscaling and regionalizing hydraulic conductivity and effective porosity at watershed scale in deeply weathered crystalline aquifers. *Journal of Hydrology*. 416. 83-97.
- Farkas-Karay, Gyöngyi & Hajnal, Géza. (2015). Modelling of Groundwater Flow in Fractured Rocks. *Procedia Environmental Sciences*. 25.
- Flerchinger, G.N., Pierson, F.B., 1991. Modeling plant canopy effects on variability of soil temperature and water. *Agricultural and Forest Meteorology* 56, 227–246.
- Freeze, F.A. and Banner, J. (1970). The mechanism of natural ground-water recharge and discharge. Laboratory Column Experiments and Field Measurements. *Water Resources Research*. 6(1):138-155.
- Freeze, R., and J. Cherry. (1979). *Groundwater*. Old Tappan, New Jersey: Prentice-Hall.
- G Cook, Peter. (2003). *A Guide to Regional Groundwater Flow in Fractured Rock Aquifers*.

- Gee, G.W. and Hillel, D. (1988) Groundwater Recharge in Arid Regions: *Review and Critique of Estimation Methods. Hydrological Processes*, 2, 255-266.
- Gleeson, T., Novakowski, K., & Kurt Kyser, T. (2009). Extremely rapid and localized recharge to a fractured rock aquifer. *Journal of Hydrology*, 376(3–4), 496–509.
- Gleeson T, Smith L, Moosdorf N, Hartmann J, Duërr HH, Manning AH, van Beek LPH, Jellinek AM (2011) Mapping permeability over the surface of the Earth. *Geophysical Research Letters*, 38, L02401.
- Gleeson, T., Wada. Y., Bierkens, M.F.P., van Beek, L.P.H. (2012). Water balance of global aquifers revealed by groundwater footprint. *Nature*, 488 (7410), pp. 197-200.
- Guymon, G.L., 1994. *Unsaturated zone hydrology*, Prentice Hall, Englewood Cliffs, New Jersey, 210 pp.
- Harbaugh, A.W.. (2005). MODFLOW-2005, the U.S. Geological survey modular ground-water model - The ground-water flow process. *U.S. Geol. Surv. Tech. Methods*.
- Harte, P.T., and Winter, T.C., 1996, Factors affecting recharge to crystalline rock in the Mirror Lake area, Grafton County, New Hampshire, in Morganwalp, D.W., ed., U.S. Geological Survey Toxics Substances Program: Proceedings of the technical meeting, Colorado Springs, Colorado, September 1993: *U.S. Geological Survey Water Resources Investigations Report 94-4015*, 12p.
- Haverkamp, R., Debionne, S., Viallet, P., Angulo-Jaramillo, R. & de Condappa, D. (2006). Soil properties and moisture movement in the unsaturated zone: 6.1-6.59. In J.W. Delleur (ed.), *The handbook of Ground-water Engineering*. CRC: Boca Raton.
- Healy RW (2010) *Estimating groundwater recharge*, Cambridge University Press, Cambridge
- Hewlett, J.D. and Hibbert, A.R. 1967: Factors affecting the response of small watersheds to precipitation in humid areas. In *Sopper, W.E. and Lull, H.W., editors, Forest hydrology*, New York: Pergamon Press, 275—90.
- Hornberger, G. M., J. P. Raffensperger, P. L. Wiberg, and K. N. Eshleman, 1998: *Elements of Physical Hydrology*. The Johns Hopkins University Press, 302 pp.



- Jiménez-Martínez, J., Longuevergne, L., Le Borgne, T., Davy, P., Russian, A., & Bour, O. (2013). Temporal and spatial scaling of hydraulic response to recharge in fractured aquifers: Insights from a frequency domain analysis. *Water Resources Research*, 49(5), 3007–3023.
- Lamur, Anthony & Kendrick, Jackie & Eggertsson, Guðjón & J. Wall, R & D. Ashworth, J & Lavallée, Yan. (2017). The permeability of fractured rocks in pressurised volcanic and geothermal systems. *Scientific Reports*. 7.
- Le Borgne, T., Bour, O., de Dreuzy, J. R., Davy, P., and Touchard, F. (2004), Equivalent mean flow models for fractured aquifers: Insights from a pumping tests scaling interpretation, *Water Resour. Res.*, 40, W03512.
- Le Borgne, T., Bour, O., Paillet, F. L., & Caudal, J. P. (2006). Assessment of preferential flow path connectivity and hydraulic properties at single-borehole and cross-borehole scales in a fractured aquifer. *Journal of Hydrology*, 328(1–2), 347–359.
- Le Borgne, T., Paillet, F., Bour, O., & Caudal, J. P. (2006). Cross-borehole flowmeter tests for transient heads in heterogeneous aquifers. *Ground Water*, 44(3), 444–452.
- Le Borgne, T, Bour, O, Riley, M, Gouze, P, Belgouhl, A, Lods, G, Le Provost, R, Greswell, R, Ellis, PA, Isakov, E, Last, B & Pezard, PJ. (2007). Comparison of alternative methodologies for identifying and characterizing preferential flow paths in heterogeneous aquifers. *Journal of Hydrology*, 345(3-4), pp. 134-148.
- Le Druillennec, Thomas & Ielsch, Geraldine & Bour, Olivier & Tarits, Corinne & Tymen, Georges & Alcalde, G & Aquilina, Luc. (2010). Hydrogeological and geochemical control of the variations of <sup>222</sup>Rn concentrations in a hard rock aquifer: Insights into the possible role of fracture-matrix exchanges. *Applied Geochemistry*. 25. 345-356.
- Lee, L.J.E., Lawrence, D.S.L., & Price, M. (2006). Analysis of water-level response to rainfall and implications for recharge pathways in the Chalk aquifer, SE England. *J. Hydrol.* 330. 604–20
- Leray, S., de Dreuzy, J. R., Bour, O., Labasque, T., & Aquilina, L. (2012). Contribution of age data to the characterization of complex aquifers. *Journal of Hydrology*, 464–465(December 2017), 54–68.

- Leray, S., de Dreuzy, J. R., Bour, O., & Bresciani, E. (2013). Numerical modeling of the productivity of vertical to shallowly dipping fractured zones in crystalline rocks. *Journal of Hydrology*, 481, 64–75.
- Lerner, D.N., Issar, S.A., & Simmers, I. (1990). Groundwater recharge – a guide to understanding and estimating natural recharge. *Heise, Hannover*, 345 pp.
- Lerner, D.N. (2002). Identifying and quantifying urban recharge: A review. *Hydrogeology Journal*, 10, pp. 143-152.
- Lloyd, J. W. (1986). *A review of aridity and groundwater*. *Hydrol. Process.*, 1: 63-78.
- Mustafa, S.M.T., Abdollahi, K., Verbeiren, B., Huysmans, M. (2017a). Identification of the influencing factors on groundwater drought and depletion in northwestern Bangladesh. *Hydrogeol. J.* 1–19.
- Nimmo, J.R. (2005). Unsaturated Zone Flow Processes, in Anderson, M.G., and Bear, J., eds., *Encyclopedia of Hydrological Sciences: Part 13--Groundwater*: Chichester, UK, Wiley, v. 4, p. 2299-2322.
- Niswonger, R.G., D.E. Prudic, and R.S. Regan. 2006. Documentation of the Unsaturated-Zone Flow (UZFI) Package for modeling unsaturated flow between the land surface and the water table with MODFLOW-2005. *USGS Techniques and Methods 6-A19*. Reston, Virginia: USGS.
- Niswonger, R.G., Panday, S., Ibaraki, M. (2011). MODFLOW-NWT, A Newton formulation for MODFLOW-2005: *U.S. Geological Survey Techniques and Methods 6-A37*, 44 p
- Pedretti, D., Russian, A., Sanchez-Vila, X., and Dentz, M. (2016), Scale dependence of the hydraulic properties of a fractured aquifer estimated using transfer functions, *Water Resour. Res.*, 52, 5008– 5024.
- Rodhe, A., 1987. The origin of streamwater traced by oxygen-18, Ph.D. thesis, Report Series A No. 41. Division of Hydrology. *Department of Physical Geography. Uppsala University, Sweden*, 260 pp.
- Roques, C & Bour, Olivier & Aquilina, Luc & Dewandel, Benoit. (2016). High-yielding aquifers in crystalline basement: insights about the role of fault zones, exemplified by Armorican Massif, France. *Hydrogeology Journal*.

- Roques, C & Aquilina, Luc & Boisson, Alexandre & Vergnaud-Ayraud, Virginie & Labasque, T & Longuevergne, Laurent & Laurencelle, Marc & Dufresne, Alexis & de Dreuzy, Jean-Raynald & Pauwels, Hélène & Bour, Olivier. (2018). Autotrophic denitrification supported by biotite dissolution in crystalline aquifers: (2) transient mixing and denitrification dynamic during long-term pumping. *The Science of the total environment*. 619-620. 491-503.
- Ruelleu, S., Moreau, F., Bour, O., Gapais, D., & Martelet, G. (2010). Impact of gently dipping discontinuities on basement aquifer recharge: An example from Ploemeur (Brittany, France). *Journal of Applied Geophysics*, 70(2), 161–168.
- Scanlon, Bridget & Healy, Richard & G. Cook, Peter. (2002). Choosing Appropriate Techniques for Quantifying Groundwater Recharge. *Hydrogeology Journal*. 10. 18-39.
- Schuite, J., Longuevergne, L., Bour, O., Burbey, T. J., Boudin, F., Lavenant, N., & Davy, P. (2017). Understanding the hydromechanical behavior of a fault zone from transient surface tilt and fluid pressure observations at hourly time scales. *Water Resources Research*, 53,10,558– 10,582.
- Schuite, Jonathan & Longuevergne, Laurent & Bour, Olivier & Boudin, F & Durand, Stéphane & Lavenant, Nicolas. (2015). Inferring field-scale properties of a fractured aquifer from ground surface deformation during a well test. *Geophysical Research Letters*. 42.
- Sklash, Michael G. & Farvolden, Robert N. (1979). The Role of Groundwater in Storm Runoff. *Journal of Hydrology*. 43. 45-65.
- Stober I, Bucher K (2006) Hydraulic properties of the crystalline basement. *Hydrogeology Journal*, 15, 213–24.
- Sukhija BS, Reddy DV, Nagabhushanam P, Hussain S. (2003). Recharge processes: piston flow vs. preferential flow in semi-arid aquifers of India. *Hydrogeol J* 11(3): 387–395
- Tolman, C.F., *Ground Water*, McGraw-Hill, New York, 1937, 593 pp., 175.
- Vergnaud-Ayraud, Virginie & Aquilina, Luc & Labasque, T & Pauwels, Hélène & Molenat, Jérôme & Pierson-Wickmann, Anne-Catherine & Durand, Véronique & Bour, Olivier & Tarits, Corinne & Le Corre, Pierre & Fourré, Elise & Merot, Philippe & Davy, Philippe. (2008). Compartmentalization of physical and chemical properties in hard-rock aquifers deduced from chemical and groundwater age analyses. *Applied*

*Geochemistry*, 23, 2686-2707.

- Wakode, H.B., Baier, K., Jha, R., & Azzam, R. (2018). Impact of urbanization on groundwater recharge and urban water balance for the city of Hyderabad, India. *International Soil and Water Conservation Research*, 6, 1.
- Widodo, Lilik Eko. (2013). Estimation of Natural Recharge and Groundwater Build up in the Bandung Groundwater Basin Contributed from Rain Water Infiltration and Inter-aquifer Transfer. *Procedia Earth and Planetary Science*, 6, 187-194.
- Winston, R.B., 2009, ModelMuse—A graphical user interface for MODFLOW–2005 and PHAST: *U.S. Geological Survey Techniques and Methods 6–A29*, 52 p
- Winter, T.C. & Harvey, J.W. & Lehn Franke, O & Alley, William. (1998). Ground water and surface water a single resource: *U. U.S. Geol. Surv. Circ.. 1139*
- Zimmermann, U & Ehhalt, D & Muennich, K.O.. (1967). Soil-water movement and evapotranspiration: changes in the isotopic composition of the water. *Isotopes in Hydrology*, pp 567-85. Vienna, International Atomic Energy Agency, 14–18.